

Self-Supervised Aggregation of Diverse Experts for Test-Agnostic Long-Tailed Recognition

Yifan Zhang¹ Bryan Hooi¹ Lanqing Hong² Jiashi Feng³
¹National University of Singapore ²Huawei Noah's Ark Lab ³ByteDance
yifan.zhang@u.nus.edu, jshfeng@gmail.com

Abstract

Existing long-tailed recognition methods, aiming to train class-balanced models from long-tailed data, generally assume the models would be evaluated on the uniform test class distribution. However, practical test class distributions often violate this assumption (*e.g.*, being either long-tailed or even inversely long-tailed), which may lead existing methods to fail in real applications. In this paper, we study a more practical yet challenging task, called *test-agnostic long-tailed recognition*, where the training class distribution is long-tailed while the test class distribution is *agnostic and not necessarily uniform*. In addition to the issue of class imbalance, this task poses another challenge: the class distribution shift between the training and test data is unknown. To tackle this task, we propose a novel approach, called *Self-supervised Aggregation of Diverse Experts*, which consists of two strategies: (i) a new skill-diverse expert learning strategy that trains multiple experts from a single and stationary long-tailed dataset to separately handle different class distributions; (ii) a novel test-time expert aggregation strategy that leverages self-supervision to aggregate the learned multiple experts for handling unknown test class distributions. We theoretically show that our self-supervised strategy has a provable ability to simulate test-agnostic class distributions. Promising empirical results demonstrate the effectiveness of our method on both vanilla and test-agnostic long-tailed recognition. Code is available at <https://github.com/Vanint/SADE-AgnosticLT>.

1 Introduction

Real-world visual recognition datasets typically exhibit a long-tailed distribution, where a few classes contain numerous samples (called head classes), but the others are associated with only a few instances (called tail classes) [24, 33]. Due to the class imbalance, the trained model is easily biased towards head classes and perform poorly on tail classes [2, 58]. To tackle this issue, numerous studies have explored long-tailed recognition for learning well-performing models from imbalanced data [20, 56].

Most existing long-tailed studies [3, 9, 10, 48, 52] assume the test class distribution is uniform, *i.e.*, each class has an equal amount of test data. Therefore, they develop various techniques, *e.g.*, class re-sampling [13, 18, 25, 55], cost-sensitive learning [11, 36, 41, 47] or ensemble learning [2, 13, 27, 53], to re-balance the model performance on different classes for fitting the uniform class distribution. However, this assumption does not always hold in real applications, where actual test data may follow any kind of class distribution, being either uniform, long-tailed, or even inversely long-tailed to the training data (cf. Figure 1(a)). For example, one may train a recognition model for autonomous cars based on the training data collected from city areas, where pedestrians are majority classes and stone obstacles are minority classes. However, when the model is deployed to mountain areas, the pedestrians become the minority while the stones become the majority. In this case, the test class distribution is inverse to the training one, and existing methods may perform poorly.

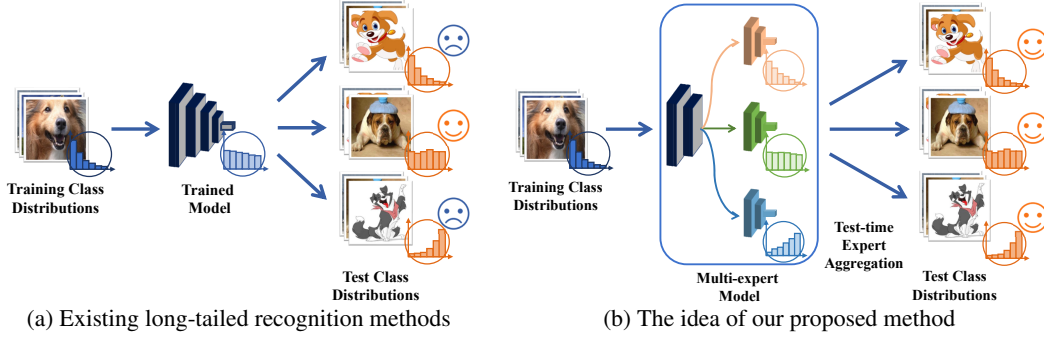


Figure 1: Illustration of test-agnostic long-tailed recognition. (a) Existing long-tailed recognition methods aim to train models that perform well on test data with the uniform class distribution. However, the resulting models may fail to handle practical test class distributions that skew arbitrarily. (b) Our method seeks to learn a multi-expert model from a single long-tailed training set, where different experts are skilled in handling different class distributions, respectively. By reasonably aggregating these experts at test time, our method is able to handle unknown test class distributions.

To address the issue of varying class distributions, as the first research attempt, LADE [17] assumes the test class distribution to be known and uses the knowledge to post-adjust model predictions. However, the actual test class distribution is usually unknown a priori, making LADE not applicable in practice. Therefore, we study a more realistic yet challenging problem, namely *test-agnostic long-tailed recognition*, where the training class distribution is long-tailed while the test distribution is *agnostic*. To tackle this problem, motivated by the idea of "divide and conquer", we propose to learn multiple experts with *diverse* skills that excel at handling different class distributions (cf. Figure 1(b)). As long as these skill-diverse experts can be aggregated suitably at test time, the multi-expert model would manage to handle the unknown test class distribution. Following this idea, we develop a novel approach, namely *Self-supervised Aggregation of Diverse Experts* (SADE).

The first challenge for SADE is how to learn multiple *diverse* experts from a *single* and *stationary* long-tailed training dataset. To handle this challenge, we empirically evaluate existing long-tailed methods in this task, and find that the models trained by existing methods have a *simulation correlation between the learned class distribution and the training loss function*. That is, the models learned by various losses are skilled in handling class distributions with different skewness. For example, the model trained with the conventional softmax loss simulates the long-tailed training class distribution, while the models obtained from existing long-tailed methods are good at the uniform class distribution. Inspired by this finding, SADE presents a simple but effective skill-diverse expert learning strategy to generate experts with different distribution preferences from a single long-tailed training distribution. Here, various experts are trained with different expertise-guided objective functions to deal with different class distributions, respectively. As a result, the learned experts are more diverse than previous multi-expert long-tailed methods [49, 63], leading to better ensemble performance, and in aggregate simulate a wide spectrum of possible class distributions.

The other challenge is how to aggregate these skill-diverse experts for handling test-agnostic class distributions based on only *unlabeled test data*. To tackle this challenge, we empirically investigate the property of different experts, and observe that there is a *positive correlation between expertise and prediction stability*, i.e., stronger experts have higher prediction consistency between different perturbed views of samples from their favorable classes. Motivated by this finding, we develop a novel self-supervised strategy, namely prediction stability maximization, to adaptively aggregate experts based on only unlabeled test data. We theoretically show that maximizing the prediction stability enables SADE to learn an aggregation weight that maximizes the mutual information between the predicted label distribution and the true class distribution. In this way, the resulting model is able to simulate unknown test class distributions.

We empirically verify the superiority of SADE on both vanilla and test-agnostic long-tailed recognition. Specifically, SADE achieves promising performance on vanilla long-tailed recognition under all benchmark datasets. For instance, SADE achieves 58.8% accuracy on ImageNet-LT with more than 2% accuracy gain over previous state-of-the-art ensemble long-tailed methods, i.e., RIDE [49] and ACE [2]. More importantly, SADE is the first long-tailed approach that is able to handle various test-agnostic class distributions without knowing the true class distribution of test data in advance. Note that SADE even outperforms LADE [17] that uses knowledge of the test class distribution.

Compared to previous long-tailed methods (*e.g.*, LADE [17] and RIDE [49]), our method offers the following advantages: (i) SADE does not assume the test class distribution to be known, and provides the first practical approach to handling test-agnostic long-tailed recognition; (ii) SADE develops a simple diversity-promoting strategy to learn skill-diverse experts from a single and stationary long-tailed dataset; (iii) SADE presents a novel self-supervised strategy to aggregate skill-diverse experts at test time, by maximizing prediction consistency between unlabeled test samples’ perturbed views; (iv) the presented self-supervised strategy has a provable ability to simulate test-agnostic class distributions, which opens the opportunity for tackling unknown class distribution shifts at test time.

2 Related Work

Long-tailed recognition Existing long-tailed recognition methods, related to our study, can be categorized into three types: class re-balancing, logit adjustment and ensemble learning. Specifically, class re-balancing resorts to re-sampling [4, 13, 18, 25] or cost-sensitive learning [3, 10, 16, 61] to balance different classes during model training. Logit adjustment [17, 33, 37, 43] adjusts models’ output logits via the label frequencies of training data at inference time, for obtaining a large relative margin between head and tail classes. Ensemble-based methods [2, 13, 53, 63], *e.g.*, RIDE [49], are based on multiple experts, which seek to capture heterogeneous knowledge, followed by ensemble aggregation. More discussions on the difference between our method and RIDE [49] are provided in Appendix D.3. Regarding test-agnostic long-tailed recognition, LADE [17] assumes the test class distribution is available and uses it to post-adjust model predictions. However, the true test class distribution is usually unknown a priori, making LADE inapplicable. In contrast, our method does not rely on the true test distribution for handling this problem, but presents a novel self-supervised strategy to aggregate skill-diverse experts at test time for test-agnostic class distributions. Moreover, some ensemble-based long-tailed methods [39] aggregate experts based on a *labeled* uniform validation set. However, as the test class distribution could be different from the validation one, simply aggregating experts on the validation set is unable to handle test-agnostic long-tailed recognition.

Test-time training Test-time training [23, 26, 30, 40, 46] is a transductive learning paradigm for handling distribution shifts [28, 32, 34, 38, 45, 59] between training and test data, and has been applied with success to out-of-domain generalization [19, 35] and dynamic scene deblurring [6]. In this study, we explore this paradigm to handle test-agnostic long-tailed recognition, where the issue of class distribution shifts is the main challenge. However, most existing test-time training methods seek to handle covariate distribution shifts instead of class distribution shifts, so simply leveraging them cannot resolve test-agnostic long-tailed recognition, as shown in our experiment (cf. Table 9).

3 Problem Formulation

Long-tailed recognition aims to learn a well-performing classification model from a training dataset with long-tailed class distribution. Let $\mathcal{D}_s = \{x_i, y_i\}_{i=1}^{n_s}$ denote the long-tailed training set, where y_i is the class label of the sample x_i . The total number of training data over C classes is $n_s = \sum_{k=1}^C n_k$, where n_k denotes the number of samples in class k . Without loss of generality, we follow a common assumption [17, 25] that the classes are sorted by cardinality in decreasing order (*i.e.*, if $i_1 < i_2$, then $n_{i_1} \geq n_{i_2}$), and $n_1 \gg n_C$. The imbalance ratio is defined as $\max(n_k)/\min(n_k) = n_1/n_C$. The test data $\mathcal{D}_t = \{x_j, y_j\}_{j=1}^{n_t}$ is defined in a similar way.

Most existing long-tailed recognition methods assume the test class distribution is uniform (*i.e.*, $p_t(y) = 1/C$), and seek to train models from the long-tailed training distribution $p_s(y)$ to perform well on the uniform test distribution. However, such an assumption does not always hold in practice. The actual test class distribution in real-world applications may also be long-tailed (*i.e.*, $p_t(y) = p_s(y)$), or even inversely long-tailed to the training data (*i.e.*, $p_t(y) = \text{inv}(p_s(y))$). Here, $\text{inv}(\cdot)$ indicates that the order of the long tail on classes is flipped. As a result, the models learned by existing methods may fail when the actual test class distribution is different from the assumed one. To address this, we propose to study a more practical yet challenging long-tailed problem, *i.e.*, **Test-agnostic Long-tailed Recognition**. This task aims to learn a recognition model from long-tailed training data, where the resulting model would be evaluated on multiple test sets that follow different class distributions. This task is challenging due to the integration of two challenges: (1) the severe class imbalance in the training data makes it difficult to train models; (2) unknown class distribution shifts between training and test data (*i.e.*, $p_t(y) \neq p_s(y)$) makes models hard to generalize.

Table 1: Accuracy of existing long-tailed (LT) methods on ImageNet-LT with various test class distributions, including uniform, forward and backward LT distributions with imbalance ratios of 10 and 50, respectively. The results show that each method strives to simulate a specific class distribution in terms of many-shot, medium-shot and few-shot classes, which does not change when the test class distribution varies. The corresponding visualization results are reported in Figure 5 in Appendix D.4.

Test class distribution	Softmax			Balanced Softmax [21]			LADE w/o prior [17]		
	Many	Medium	Few	Many	Medium	Few	Many	Medium	Few
Forward-LT-50	67.5	41.7	14.0	63.5	47.8	37.5	63.5	46.4	33.1
Forward-LT-10	68.2	40.9	14.0	64.1	48.2	31.2	64.7	47.1	32.2
Uniform	68.1	41.5	14.0	64.1	48.2	33.4	64.4	47.7	34.3
Backward-LT-10	67.4	41.9	13.9	63.4	49.1	33.6	64.4	48.2	34.2
Backward-LT-50	70.9	41.1	13.8	66.5	48.4	33.2	66.3	47.8	34.0

4 Method

To tackle the above problem, inspired by the idea of "divide and conquer", we propose to learn multiple skill-diverse experts that excel at handling different class distributions. By reasonably fusing these experts at test time, the multi-expert model would manage to handle unknown class distribution shifts and resolve test-agnostic long-tailed recognition. Following this idea, we develop a novel Self-supervised Aggregation of Diverse Experts (SADE) approach. Specifically, SADE consists of two innovative strategies: (1) *learning skill-diverse experts* from a single long-tailed training dataset; (2) *test-time aggregating experts with self-supervision* to handle test-agnostic class distributions.

4.1 Skill-diverse Expert Learning

As shown in Figure 2, SADE builds a three-expert model that comprises two components: (1) an expert-shared backbone f_θ ; (2) independent expert networks E_1 , E_2 and E_3 . When training the model, the key challenge is how to learn skill-diverse experts from a single and stationary long-tailed training dataset. Existing ensemble-based long-tailed methods [13, 49] seek to train experts for the uniform test class distribution, and hence the trained experts are not differentiated sufficiently for handling various class distributions (refer to Table 6 for an example). To tackle this challenge, we first empirically investigate existing long-tailed methods in this task. From Table 1, we find that there is a *simulation correlation between the learned class distribution and the training loss function*. That is, the models learned by different losses are good at dealing with class distributions with different skewness. For instance, the model trained with the softmax loss is good at the long-tailed distribution, while the models obtained from long-tailed methods are skilled in the uniform distribution.

Motivated by this finding, we develop a simple skill-diverse expert learning strategy to generate experts with different distribution preferences. To be specific, the forward expert E_1 seeks to be good at the long-tailed class distribution and performs well on many-shot classes. The uniform expert E_2 strives to be skilled in the uniform distribution. The backward expert E_3 aims at the inversely long-tailed distribution and performs well on few-shot classes. Here, the forward and backward experts are necessary since they span a wide spectrum of possible class distributions, while the uniform expert ensures retaining high accuracy on the uniform distribution. To this end, we use three different expertise-guided losses to train the three experts, respectively.

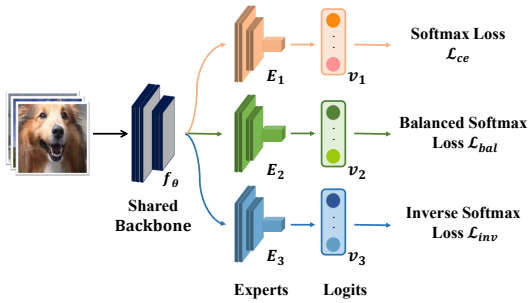


Figure 2: The scheme of SADE with three experts, where different experts are trained with different expertise-guided losses.

The forward expert E_1 We use the softmax cross-entropy loss to train this expert, so that it directly simulates the original long-tailed training class distribution:

$$\mathcal{L}_{ce} = \frac{1}{n_s} \sum_{x_i \in \mathcal{D}_s} -y_i \log \sigma(v_1(x_i)), \quad (1)$$

where $v_1(\cdot)$ is the output logits of the forward expert E_1 , and $\sigma(\cdot)$ is the softmax function.

The uniform expert E_2 We aim to train this expert to simulate the uniform class distribution. Inspired by the effectiveness of logit adjusted losses for long-tailed recognition [33], we resort to the balanced softmax loss [21]. Specifically, let $\hat{y}^k = \frac{\exp(v^k)}{\sum_{c=1}^C \exp(v^c)}$ be the prediction probability. The balanced softmax adjusts the prediction probability by compensating for the long-tailed class distribution with the prior of training label frequencies: $\hat{y}^k = \frac{\pi^k \exp(v^k)}{\sum_{c=1}^C \pi^c \exp(v^c)} = \frac{\exp(v^k + \log \pi^k)}{\sum_{c=1}^C \exp(v^c + \log \pi^c)}$, where $\pi^k = \frac{n_k}{n}$ denotes the training label frequency of class k . Then, given $v_2(\cdot)$ as the output logits of the expert E_2 , the balanced softmax loss for the expert E_2 is defined as:

$$\mathcal{L}_{bal} = \frac{1}{n_s} \sum_{x_i \in \mathcal{D}_s} -y_i \log \sigma(v_2(x_i) + \log \pi). \quad (2)$$

Intuitively, by adjusting logits to compensate for the long-tailed distribution with the prior π , this loss enables E_2 to output class-balanced predictions that simulate the uniform distribution.

The backward expert E_3 We seek to train this expert to simulate the inversely long-tailed class distribution. To this end, we propose a new *inverse softmax loss*, based on the same rationale of logit adjusted losses [21, 33]. Specifically, we adjust the prediction probability by: $\hat{y}^k = \frac{\exp(v^k + \log \pi^k - \log \bar{\pi}^k)}{\sum_{c=1}^C \exp(v^c + \log \pi^c - \log \bar{\pi}^c)}$, where the inverse training prior $\bar{\pi}$ is obtained by inverting the order of training label frequencies π . Then, the new inverse softmax loss for the expert E_3 is defined as:

$$\mathcal{L}_{inv} = \frac{1}{n_s} \sum_{x_i \in \mathcal{D}_s} -y_i \log \sigma(v_3(x_i) + \log \pi - \lambda \log \bar{\pi}), \quad (3)$$

where $v_3(\cdot)$ denotes the output logits of E_3 and λ is a hyper-parameter. Intuitively, this loss adjusts logits to compensate for the long-tailed distribution with π , and further applies reverse adjustment with $\bar{\pi}$. This enables E_3 to simulate the inversely long-tailed distribution (cf. Table 6 for verification).

4.2 Test-time Self-supervised Aggregation

Based on the skill-diverse learning strategy, the three experts in SADE are skilled in different class distributions. The remaining challenge is how to fuse them to deal with unknown test class distributions. A basic principle for expert aggregation is that the experts should play a bigger role in situations where they have expertise. Nevertheless, how to detect strong experts for unknown test class distribution remains unknown. Our key insight is that strong experts should be more stable in predicting the samples from their skilled classes, even though these samples are perturbed.

Empirical observation To verify this hypothesis, we estimate the prediction stability of experts by comparing the cosine similarity between their predictions for a sample’s two augmented views. Here, the data views are generated by the data augmentation techniques in MoCo v2 [5]. From Table 2, we find that there is a *positive correlation between expertise and prediction stability*, i.e., stronger experts have higher prediction similarity between different views of samples from their favorable classes. Following this finding, we propose to explore the relative prediction stability to detect strong experts and weight experts for the unknown test class distribution. Consequently, we develop a novel self-supervised strategy, namely prediction stability maximization.

Prediction stability maximization This strategy learns aggregation weights for experts (with frozen parameters) by maximizing model prediction stability for unlabeled test samples. As shown in Figure 3, the method comprises three major components as follows.

Data view generation For a given sample x , we conduct two stochastic data augmentations to generate the sample’s two views, i.e., x^1 and x^2 . Here, we use the same augmentation techniques as the advanced contrastive learning method, i.e., MoCo v2 [5], which has been shown effective in self-supervised learning.

Learnable aggregation weight Given the output logits of three experts $(v_1, v_2, v_3) \in \mathbb{R}^{3 \times C}$, we aggregate experts with a learnable aggregation weight $w = [w_1, w_2, w_3] \in \mathbb{R}^3$ and obtain the final softmax prediction by $\hat{y} = \sigma(w_1 \cdot v_1 + w_2 \cdot v_2 + w_3 \cdot v_3)$, where w is normalized before aggregation, i.e., $w_1 + w_2 + w_3 = 1$.

Table 2: Prediction stability of experts in terms of the cosine similarity between their predictions of a sample’s two views. Note that expert E_1 is good at many-shot classes and expert E_3 is skilled in few-shot classes. The experts tend to have better prediction consistency for the samples from their skilled classes. Here, the imbalance ratio of CIFAR100-LT is 100.

Model	Cosine similarity between view predictions					
	ImageNet-LT			CIFAR100-LT		
	Many	Med.	Few	Many	Med.	Few
Expert E_1	0.60	0.48	0.43	0.28	0.22	0.20
Expert E_2	0.56	0.50	0.45	0.25	0.21	0.19
Expert E_3	0.52	0.53	0.58	0.22	0.23	0.25

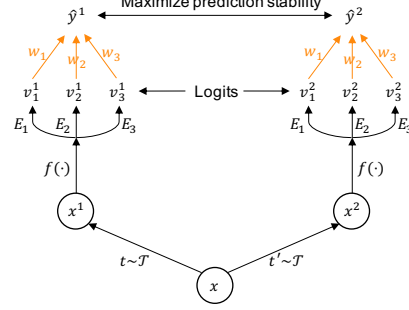


Figure 3: The scheme of test-time self-supervised aggregation. Two data augmentations sampled from the same family of augmentations ($t \sim \mathcal{T}$ and $t' \sim \mathcal{T}$) are applied to obtain two data views.

Objective function Given the view predictions of unlabeled test data, we maximize the prediction stability based on the cosine similarity between the view predictions:

$$\max_w \mathcal{S}, \text{ where } \mathcal{S} = \frac{1}{n_t} \sum_{x \in \mathcal{D}_t} \hat{y}^1 \cdot \hat{y}^2. \quad (4)$$

Here, \hat{y}^1 and \hat{y}^2 are normalized by the softmax function. In test-time training, only the aggregation weight w is updated. Since stronger experts have higher prediction similarity for their skilled classes, maximizing the prediction stability \mathcal{S} would learn higher weights for stronger experts regarding the unknown test class distribution. Moreover, the self-supervised aggregation strategy can be conducted in an online manner for streaming test data. The pseudo-code of SADE is provided in Appendix B.

Theoretical Analysis We then theoretically analyze the prediction stability maximization strategy to conceptually understand why it works. To this end, we first define the random variables of predictions and labels as $\hat{Y} \sim p(\hat{y})$ and $Y \sim p_t(y)$. We have the following result:

Theorem 1. *The prediction stability \mathcal{S} is positive proportional to the mutual information between the predicted label distribution and the test class distribution $I(\hat{Y}; Y)$, and negative proportional to the prediction entropy $H(\hat{Y})$:*

$$\mathcal{S} \propto I(\hat{Y}; Y) - H(\hat{Y}).$$

Please refer to Appendix A for proofs. According to Theorem 1, maximizing the prediction stability \mathcal{S} enables SADE to learn an aggregation weight that maximizes the mutual information between the predicted label distribution $p(\hat{y})$ and the test class distribution $p_t(y)$, as well as minimizing the prediction entropy. Since minimizing entropy helps to improve the confidence of the classifier output [12], the aggregation weight is learned to simulate the test class distribution $p_t(y)$ and increase the prediction confidence. This property intuitively explains why our method has the potential to tackle the challenging task of test-agnostic long-tailed recognition at test time.

5 Experiments

In this section, we first evaluate the superiority of SADE on both vanilla and test-agnostic long-tailed recognition. We then verify the effectiveness of SADE in terms of its two strategies, *i.e.*, skill-diverse expert learning and test-time self-supervised aggregation. More ablation studies are reported in appendices. Here, we begin with the experimental settings.

5.1 Experimental Setups

Datasets We use four benchmark datasets (*i.e.*, ImageNet-LT [31], CIFAR100-LT [3], Places-LT [31], and iNaturalist 2018 [44]) to simulate real-world long-tailed class distributions. Their data statistics and imbalance ratios are summarized in Appendix C.1. The imbalance ratio is defined as $\max n_j / \min n_j$, where n_j denotes the data number of class j . Note that CIFAR100-LT has three variants with different imbalance ratios.

Table 3: Top-1 accuracy on CIFAR100-LT, Places-LT and iNaturalist 2018, where the test class distribution is uniform. More results on three class sub-groups are reported in Appendix D.1.

(a) CIFAR100-LT				(b) Places-LT		(c) iNaturalist 2018	
Imbalance Ratio	10	50	100	Method	Top-1 accuracy	Method	Top-1 accuracy
Softmax	59.1	45.6	41.4	Softmax	31.4	Softmax	64.7
BBN [63]	59.8	49.3	44.7	Causal [42]	32.2	Causal [42]	64.4
Causal [42]	59.4	48.8	45.0	Balanced Softmax [21]	39.4	Balanced Softmax [21]	70.6
Balanced Softmax [21]	61.0	50.9	46.1	MiSLAS [62]	38.3	MiSLAS [62]	70.7
MiSLAS [62]	62.5	51.5	46.8	LADE [17]	39.2	LADE [17]	69.3
LADE [17]	61.6	50.1	45.6	RIDE [49]	40.3	RIDE [49]	71.8
RIDE [49]	61.8	51.7	48.0	SADE (ours)	40.9	SADE (ours)	72.9

Baselines We compare SADE with state-of-the-art long-tailed methods, including two-stage methods (Decouple [25], MiSLAS [62]), logit-adjusted training (Balanced Softmax [21], LADE [17]), ensemble learning (BBN [63], ACE [2], RIDE [49]), classifier design (Causal [42]), and representation learning (PaCo [8]). Note that LADE uses the prior of test class distribution for post-adjustment (although it is unavailable in practice), while all other methods do not use this prior.

Evaluation protocols In test-agnostic long-tailed recognition, following LADE [17], the models are evaluated on multiple sets of test data that follow different class distributions, in terms of micro accuracy. Same as LADE [17], we construct three kinds of test class distributions, *i.e.*, the uniform distribution, forward long-tailed distributions as training data, and backward long-tailed distributions. In the backward ones, the order of the long tail on classes is flipped. More details of test data construction are provided in Appendix C.2. Besides, we also evaluate methods on vanilla long-tailed recognition [25, 31], where the models are evaluated on the uniform test class distribution. Here, the accuracy on three class sub-groups is also reported, *i.e.*, many-shot classes (more than 100 training images), medium-shot classes (20~100 images) and few-shot classes (less than 20 images).

Implementation details We use the same setup for all the baselines and our method. Specifically, following [17, 49], we use ResNeXt-50 for ImageNet-LT, ResNet-32 for CIFAR100-LT, ResNet-152 for Places-LT and ResNet-50 for iNaturalist 2018 as backbones, respectively. Moreover, we adopt the cosine classifier for prediction on all datasets. If not specified, we use the SGD optimizer with the momentum of 0.9 for training 200 epochs and set the initial learning rate as 0.1 with linear decay. We set $\lambda=2$ for ImageNet-LT and CIFAR100-LT, and $\lambda=1$ for the remaining datasets. During test-time training, we train the aggregation weights for 5 epochs with the batch size 128, where we use the same optimizer and learning rate as the training phase. More implementation details and the hyper-parameter statistics are reported in Appendix C.3.

5.2 Superiority on Vanilla Long-tailed Recognition

This subsection compares SADE with state-of-the-art long-tailed methods on vanilla long-tailed recognition. Specifically, as shown in Tables 3-4, Softmax trains the model with only cross-entropy, so it simulates the long-tailed training distribution and performs well on many-shot classes. However, it performs poorly on medium-shot and few-shot classes, leading to worse overall performance. In contrast, existing long-tailed methods (*e.g.*, Decouple, Causal) seek to simulate the uniform class distribution, so their performance is more class-balanced, leading to better overall performance. However, as these methods mainly seek balanced performance, they inevitably sacrifice the performance on many-shot classes. To address this, RIDE and ACE explore ensemble learning for long-tailed recognition and achieve better performance on tail classes without sacrificing the head-class performance. In comparison, based on the increasing expert diversity derived from skill-diverse expert learning, our method performs the best on all datasets, *e.g.*, with more than 2% accuracy gain on ImageNet-LT compared to RIDE and ACE. These results demonstrate the superiority of SADE over the compared methods that are particularly designed for the uniform test class distribution. Note that SADE also outperforms baselines in experiments with stronger data augmentation (*i.e.*, RandAugment [7]) and other architectures, as reported in Appendix D.1.

Table 4: Top-1 accuracy on ImageNet-LT.

Method	Many	Med.	Few	All
Softmax	68.1	41.5	14.0	48.0
Decouple-LWS [25]	61.8	47.6	30.9	50.8
Causal [42]	64.1	45.8	27.2	50.3
Balanced Softmax [21]	64.1	48.2	33.4	52.3
MiSLAS [62]	62.0	49.1	32.8	51.4
LADE [17]	64.4	47.7	34.3	52.3
PaCo [8]	63.2	51.6	39.2	54.4
ACE [2]	71.7	54.6	23.5	56.6
RIDE [49]	68.0	52.9	35.1	56.3
SADE (ours)	66.5	57.0	43.5	58.8

Table 5: Top-1 accuracy on long-tailed datasets with various unknown test class distributions. “Prior” indicates that the test class distribution is used as prior knowledge. “Uni.” denotes the uniform distribution. “IR” indicates the imbalance ratio. “BS” denotes the balanced softmax [21].

		(a) ImageNet-LT												(b) CIFAR100-LT (IR100)											
Method	Prior	Forward-LT					Uni.	Backward-LT					Forward-LT					Uni.	Backward-LT						
		50	25	10	5	2	1	2	5	10	25	50	50	25	10	5	2	1	2	5	10	25	50		
Softmax	✗	66.1	63.8	60.3	56.6	52.0	48.0	43.9	38.6	34.9	30.9	27.6	63.3	62.0	56.2	52.5	46.4	41.4	36.5	30.5	25.8	21.7	17.5		
BS	✗	63.2	61.9	59.5	57.2	54.4	52.3	50.0	47.0	45.0	42.3	40.8	57.8	55.5	54.2	52.0	48.7	46.1	43.6	40.8	38.4	36.3	33.7		
MiSLAS	✗	61.6	60.4	58.0	56.3	53.7	51.4	49.2	46.1	44.0	41.5	39.5	58.8	57.2	55.2	53.0	49.6	46.8	43.6	40.1	37.7	33.9	32.1		
LADE	✗	63.4	62.1	59.9	57.4	54.6	52.3	49.9	46.8	44.9	42.7	40.7	56.0	55.5	52.8	51.0	48.0	45.6	43.2	40.0	38.3	35.5	34.0		
LADE	✓	65.8	63.8	60.6	57.5	54.5	52.3	50.4	48.8	48.6	49.0	49.2	62.6	60.2	55.6	52.7	48.2	45.6	43.8	41.1	41.5	40.7	41.6		
RIDE	✗	67.6	66.3	64.0	61.7	58.9	56.3	54.0	51.0	48.7	46.2	44.0	63.0	59.9	57.0	53.6	49.4	48.0	42.5	38.1	35.4	31.6	29.2		
SADE	✗	69.4	67.4	65.4	63.0	60.6	58.8	57.1	55.5	54.5	53.7	53.1	65.9	62.5	58.3	54.8	51.1	49.8	46.2	44.7	43.9	42.5	42.4		

		(c) Places-LT										(d) iNaturalist 2018					
Method	Prior	Forward-LT					Uni.	Backward-LT					Forward-LT		Uni.	Backward-LT	
		50	25	10	5	2	1	2	5	10	25	50	3	2	1	2	3
Softmax	✗	45.6	42.7	40.2	38.0	34.1	31.4	28.4	25.4	23.4	20.8	19.4	65.4	65.5	64.7	64.0	63.4
BS	✗	42.7	41.7	41.3	41.0	40.0	39.4	38.5	37.8	37.1	36.2	35.6	70.3	70.5	70.6	70.6	70.8
MiSLAS	✗	40.9	39.7	39.5	39.6	38.8	38.3	37.3	36.7	35.8	34.7	34.4	70.8	70.8	70.7	70.7	70.2
LADE	✗	42.8	41.5	41.2	40.8	39.8	39.2	38.1	37.6	36.9	36.0	35.7	68.4	69.0	69.3	69.6	69.5
LADE	✓	46.3	44.2	42.2	41.2	39.7	39.4	39.2	39.9	40.9	42.4	43.0	✗	69.1	69.3	70.2	✗
RIDE	✗	43.1	41.8	41.6	42.0	41.0	40.3	39.6	38.7	38.2	37.0	36.9	71.5	71.9	71.8	71.9	71.8
SADE	✗	46.4	44.9	43.3	42.6	41.3	40.9	40.6	41.1	41.4	42.0	41.6	72.3	72.5	72.9	73.5	73.3

Table 6: Performance of each expert on the uniform test distribution, where the imbalance ratio of CIFAR100-LT is 100. The results show that our proposed method learns multiple experts with higher skill diversity, which leads to better ensemble performance.

Model	RIDE [49]								SADE (ours)							
	ImageNet-LT				CIFAR100-LT				ImageNet-LT				CIFAR100-LT			
	Many	Med.	Few	All	Many	Med.	Few	All	Many	Med.	Few	All	Many	Med.	Few	All
Expert E_1	64.3	49.0	31.9	52.6	63.5	44.8	20.3	44.0	68.8	43.7	17.2	49.8	67.6	36.3	6.8	38.4
Expert E_2	64.7	49.4	31.2	52.8	63.1	44.7	20.2	43.8	65.5	50.5	33.3	53.9	61.2	44.7	23.5	44.2
Expert E_3	64.3	48.9	31.8	52.5	63.9	45.1	20.5	44.3	43.4	48.6	53.9	47.3	14.0	27.6	41.2	25.8
Ensemble	68.0	52.9	35.1	56.3	67.4	49.5	23.7	48.0	67.0	56.7	42.6	58.8	61.6	50.5	33.9	49.4

5.3 Superiority on Test-agnostic Long-tailed Recognition

In this subsection, we evaluate SADE on test-agnostic long-tailed recognition. The results on various test class distributions are reported in Table 5. Specifically, since Softmax seeks to simulate the long-tailed training distribution, it performs well on forward long-tailed test distributions. However, its performance on the uniform and backward long-tailed distributions is poor. In contrast, existing long-tailed methods show more balanced performance among classes, leading to better overall accuracy. However, the resulting models by these methods suffer from a simulation bias, *i.e.*, performing similarly among classes on various class distributions (c.f. Table 1). As a result, they cannot adapt to diverse test class distributions well. To handle this task, LADE assumes the test class distribution to be known and uses this information to adjust its predictions, leading to better performance on various test class distributions. However, since obtaining the actual test class distribution is difficult in real applications, the methods requiring such knowledge may be not applicable in practice. Moreover, in some specific cases like Forward-LT-3 and Backward-LT-3 distributions of iNaturalist 2018, the number of test samples on some classes becomes zero. In such cases, the test prior cannot be used in LADE, since adjusting logits with $\log 0$ results in biased predictions. In contrast, without relying on the knowledge of test class distributions, our SADE presents an innovative self-supervised strategy to deal with unknown class distributions, and obtains even better performance than LADE that uses the test class prior (c.f. Table 5). The promising results demonstrate the effectiveness and practicality of our method on test-agnostic long-tailed recognition. Note that the performance advantages of SADE become larger as the test data get more imbalanced. Due to the page limitation, the results on more datasets are reported in Appendix D.2.

5.4 Effectiveness of Skill-diverse Expert Learning

We next examine our skill-diverse expert learning strategy. The results are reported in Table 6, where RIDE [49] is a state-of-the-art ensemble-based method. RIDE trains each expert with cross-entropy independently and uses KL-Divergence to improve expert diversity. However, simply maximizing the divergence of expert predictions cannot learn visibly diverse experts (cf. Table 6). In contrast, the three experts learned by our strategy have significantly diverse expertise, excelling at many-shot classes, the uniform distribution (with higher overall performance), and few-shot classes, respectively. As a result, the increasing expert diversity leads to a non-trivial gain for the ensemble performance of SADE compared to RIDE. Moreover, consistent results on more datasets are reported in Appendix D.3, while the ablation studies of the expert learning strategy are provided in Appendix E.

Table 7: The expert weights learned by our self-supervised strategy on ImageNet-LT with various test class distributions. Our method learns suitable weights for various unknown distributions.

Test Dist.	Expert E_1 (w_1)	Expert E_2 (w_2)	Expert E_3 (w_3)
Forward-LT-50	0.52	0.35	0.13
Forward-LT-10	0.46	0.36	0.18
Uniform	0.33	0.33	0.34
Backward-LT-10	0.21	0.29	0.50
Backward-LT-50	0.17	0.27	0.56

Table 8: The performance improvement by our test-time self-supervised strategy on ImageNet-LT with various test class distributions.

Test Dist.	ImageNet-LT							
	Ours w/o test-time strategy				Ours w/ test-time strategy			
	Many	Med.	Few	All	Many	Med.	Few	All
Forward-LT-50	65.6	55.7	44.1	65.5	70.0	53.2	33.1	69.4 (+3.9)
Forward-LT-10	66.5	56.8	44.2	63.6	69.9	54.3	34.7	65.4 (+1.8)
Uniform	67.0	56.7	42.6	58.8	66.5	57.0	43.5	58.8 (+0.0)
Backward-LT-10	65.0	57.6	43.1	53.1	60.9	57.5	50.1	54.5 (+1.4)
Backward-LT-50	69.1	57.0	42.9	49.8	60.7	56.2	50.7	53.1 (+3.3)

Table 9: Comparison among different test-time training strategies for handling class distribution shifts on ImageNet-LT with various unknown test class distributions.

Backbone	Test-time strategy	Forward					Uniform	Backward				
		50	25	10	5	2	1	2	5	10	25	50
SADE	No test-time adaptation	65.5	64.4	63.6	62.0	60.0	58.8	56.8	54.7	53.1	51.5	49.8
	Test-time pseudo-labeling	67.1	66.1	64.7	63.0	60.1	57.7	54.7	51.1	48.1	45.0	42.4
	Test class distribution estimation [29]	69.1	66.6	63.7	60.5	56.5	53.3	49.9	45.6	42.7	39.5	36.8
	Entropy minimization with Tent [46]	68.0	67.0	65.6	62.8	60.5	58.6	56.0	53.2	50.6	48.1	45.7
	Self-supervised expert aggregation (ours)	69.4	67.4	65.4	63.0	60.6	58.8	57.1	55.5	54.5	53.7	53.1

5.5 Effectiveness of Test-time Self-supervised Aggregation

This subsection evaluates our test-time self-supervised aggregation strategy.

Effectiveness in expert aggregation. As shown in Table 7, our self-supervised strategy learns suitable expert weights for various unknown test class distributions. For forward long-tailed distributions, the weight of the forward expert E_1 is higher; while for backward long-tailed ones, the weight of the backward expert E_3 is relatively high. This enables our multi-expert model to boost the performance on dominant classes for unknown test distributions, leading to better ensemble performance (cf. Table 8), particularly as test data get more skewed. The results on more datasets are reported in Appendix D.4, while more ablation studies of our strategy are shown in Appendix F.

Superiority over test-time training methods. We then verify the superiority of our self-supervised strategy over existing test-time training approaches on various test class distributions. Specifically, we adopt three non-trivial baselines: (i) *Test-time pseudo-labeling* uses the multi-expert model to iteratively generate pseudo labels for unlabeled test data and uses them to fine-tune the model; (ii) *Test class distribution estimation* leverages BBSE [29] to estimate the test class distribution and uses it to pose-adjust model predictions; (iii) *Tent* [46] fine-tunes the batch normalization layers of models through entropy minimization on unlabeled test data. The results in Table 9 show that directly applying existing test-time training methods cannot handle well the class distribution shifts, particularly on the inversely long-tailed class distribution. In comparison, our self-supervised strategy is able to aggregate multiple experts appropriately for the unknown test class distribution (cf. Table 7), leading to promising performance gains on various test class distributions (cf. Table 9).

Effectiveness on partial class distributions.

Real-world test data may follow any type of class distribution, including partial class distributions (*i.e.*, not all of the classes appear in the test data). Motivated by this, we further evaluate SADE on three partial class distributions: only many-shot classes, only medium-shot classes, and only few-shot classes. The results in Table 10 demonstrate the effectiveness of SADE in tackling more complex test class distributions.

Table 10: The effectiveness of our self-supervised aggregation strategy in dealing with (unknown) partial test class distributions on ImageNet-LT.

Method	ImageNet-LT		
	Only many	Only medium	Only few
SADE w/o test-time strategy	67.4	56.9	42.5
SADE w/ test-time strategy	71.0	57.2	53.6
Accuracy gain	(+3.6)	(+0.3)	(+11.1)

6 Conclusion

In this paper, we have explored a practical yet challenging task of *test-agnostic long-tailed recognition*, where the test class distribution is unknown and not necessarily uniform. To tackle this task, we present a novel approach, namely *Self-supervised Aggregation of Diverse Experts* (SADE), which consists of two innovative strategies, *i.e.*, skill-diverse expert learning and test-time self-supervised aggregation. We theoretically analyze our proposed method and also empirically show that SADE achieves new state-of-the-art performance on both vanilla and test-agnostic long-tailed recognition.

Acknowledgments

This work was partially supported by NUS ODPRT Grant R252-000-A81-133 and NUS Advanced Research and Technology Innovation Centre (ARTIC) Project Reference (ECT-RP2). We also gratefully appreciate the support of MindSpore, CANN (Compute Architecture for Neural Networks) and Ascend AI Processor used for this research.

References

- [1] Malik Boudiaf, Jérôme Rony, et al. A unifying mutual information view of metric learning: cross-entropy vs. pairwise losses. In *European Conference on Computer Vision*, 2020.
- [2] Jiarui Cai, Yizhou Wang, and Jenq-Neng Hwang. Ace: Ally complementary experts for solving long-tailed recognition in one-shot. In *International Conference on Computer Vision*, 2021.
- [3] Kaidi Cao, Colin Wei, Adrien Gaidon, Nikos Arechiga, and Tengyu Ma. Learning imbalanced datasets with label-distribution-aware margin loss. In *Advances in Neural Information Processing Systems*, 2019.
- [4] Nitesh V Chawla, Kevin W Bowyer, et al. Smote: synthetic minority over-sampling technique. *Journal of Artificial Intelligence Research*, 2002.
- [5] Xinlei Chen, Haoqi Fan, Ross Girshick, and Kaiming He. Improved baselines with momentum contrastive learning. *arXiv preprint arXiv:2003.04297*, 2020.
- [6] Zhixiang Chi, Yang Wang, et al. Test-time fast adaptation for dynamic scene deblurring via meta-auxiliary learning. In *Computer Vision and Pattern Recognition*, 2021.
- [7] Ekin Dogus Cubuk, Barret Zoph, Jon Shlens, and Quoc Le. Randaugment: Practical automated data augmentation with a reduced search space. In *Advances in Neural Information Processing Systems*, volume 33, 2020.
- [8] Jiequan Cui, Zhisheng Zhong, Shu Liu, Bei Yu, and Jiaya Jia. Parametric contrastive learning. In *International Conference on Computer Vision*, 2021.
- [9] Yin Cui, Menglin Jia, et al. Class-balanced loss based on effective number of samples. In *Computer Vision and Pattern Recognition*, 2019.
- [10] Zongyong Deng, Hao Liu, Yaoxing Wang, Chenyang Wang, Zekuan Yu, and Xuehong Sun. Pml: Progressive margin loss for long-tailed age classification. In *Computer Vision and Pattern Recognition*, pages 10503–10512, 2021.
- [11] Chengjian Feng, Yujie Zhong, and Weilin Huang. Exploring classification equilibrium in long-tailed object detection. In *International Conference on Computer Vision*, 2021.
- [12] Yves Grandvalet, Yoshua Bengio, et al. Semi-supervised learning by entropy minimization. In *CAP*, 2005.
- [13] Hao Guo and Song Wang. Long-tailed multi-label visual recognition by collaborative training on uniform and re-balanced samplings. In *Computer Vision and Pattern Recognition*, 2021.
- [14] Marton Havasi, Rodolphe Jenatton, et al. Training independent subnetworks for robust prediction. In *International Conference on Learning Representations*, 2021.
- [15] Kaiming He, Xiangyu Zhang, Shaoqing Ren, and Jian Sun. Deep residual learning for image recognition. In *Computer Vision and Pattern Recognition*, pages 770–778, 2016.
- [16] Yin-Yin He, Peizhen Zhang, Xiu-Shen Wei, Xiangyu Zhang, and Jian Sun. Relieving long-tailed instance segmentation via pairwise class balance. *arXiv preprint arXiv:2201.02784*, 2022.
- [17] Youngkyu Hong, Seungju Han, Kwanghee Choi, Seokjun Seo, Beomsu Kim, and Buru Chang. Disentangling label distribution for long-tailed visual recognition. In *Computer Vision and Pattern Recognition*, 2021.
- [18] Chen Huang, Yining Li, Chen Change Loy, and Xiaoou Tang. Learning deep representation for imbalanced classification. In *Computer Vision and Pattern Recognition*, 2016.
- [19] Yusuke Iwasawa and Yutaka Matsuo. Test-time classifier adjustment module for model-agnostic domain generalization. In *Advances in Neural Information Processing Systems*, volume 34, 2021.

- [20] Muhammad Abdullah Jamal, Matthew Brown, Ming-Hsuan Yang, Liqiang Wang, and Boqing Gong. Rethinking class-balanced methods for long-tailed visual recognition from a domain adaptation perspective. In *Computer Vision and Pattern Recognition*, pages 7610–7619, 2020.
- [21] Ren Jiawei, Cunjun Yu, Xiao Ma, Haiyu Zhao, Shuai Yi, et al. Balanced meta-softmax for long-tailed visual recognition. In *Advances in Neural Information Processing Systems*, 2020.
- [22] Justin M Johnson and Taghi M Khoshgoftaar. Survey on deep learning with class imbalance. *Journal of Big Data*, 6(1):1–54, 2019.
- [23] Mohammad Mahdi Kamani, Sadegh Farhang, Mehrdad Mahdavi, and James Z Wang. Targeted data-driven regularization for out-of-distribution generalization. In *ACM SIGKDD International Conference on Knowledge Discovery & Data Mining*, pages 882–891, 2020.
- [24] Bingyi Kang, Yu Li, Sa Xie, Zehuan Yuan, and Jiashi Feng. Exploring balanced feature spaces for representation learning. In *International Conference on Learning Representations*, 2021.
- [25] Bingyi Kang, Saining Xie, Marcus Rohrbach, Zhicheng Yan, Albert Gordo, Jiashi Feng, and Yannis Kalantidis. Decoupling representation and classifier for long-tailed recognition. In *International Conference on Learning Representations*, 2020.
- [26] Ildoo Kim, Younghoon Kim, and Sungwoong Kim. Learning loss for test-time augmentation. *Advances in Neural Information Processing Systems*, 33:4163–4174, 2020.
- [27] Yu Li, Tao Wang, Bingyi Kang, Sheng Tang, Chunfeng Wang, Jintao Li, and Jiashi Feng. Overcoming classifier imbalance for long-tail object detection with balanced group softmax. In *Computer Vision and Pattern Recognition*, 2020.
- [28] Hongbin Lin, Yifan Zhang, Zhen Qiu, Shuaicheng Niu, Chuang Gan, Yanxia Liu, and Mingkui Tan. Prototype-guided continual adaptation for class-incremental unsupervised domain adaptation. In *European Conference on Computer Vision*, 2022.
- [29] Zachary Lipton, Yu-Xiang Wang, and Alexander Smola. Detecting and correcting for label shift with black box predictors. In *International conference on machine learning*, pages 3122–3130. PMLR, 2018.
- [30] Yuejiang Liu, Parth Kothari, Bastien van Delft, Baptiste Bellot-Gurlet, Taylor Mordan, and Alexandre Alahi. Ttt++: When does self-supervised test-time training fail or thrive? In *Advances in Neural Information Processing Systems*, volume 34, 2021.
- [31] Ziwei Liu, Zhongqi Miao, Xiaohang Zhan, Jiayun Wang, Boqing Gong, and Stella X Yu. Large-scale long-tailed recognition in an open world. In *Computer Vision and Pattern Recognition*, pages 2537–2546, 2019.
- [32] Mingsheng Long, Jianmin Wang, Guiguang Ding, Jiaguang Sun, and Philip S Yu. Transfer joint matching for unsupervised domain adaptation. In *Computer Vision and Pattern Recognition*, pages 1410–1417, 2014.
- [33] Aditya Krishna Menon, Sadeep Jayasumana, Ankit Singh Rawat, Himanshu Jain, Andreas Veit, and Sanjiv Kumar. Long-tail learning via logit adjustment. In *International Conference on Learning Representations*, 2021.
- [34] Shuaicheng Niu, Jiaxiang Wu, Yifan Zhang, Yaofo Chen, Shijian Zheng, Peilin Zhao, and Mingkui Tan. Efficient test-time model adaptation without forgetting. In *International conference on machine learning*, 2022.
- [35] Prashant Pandey, Mrigank Raman, Sumanth Varambally, and Prathosh AP. Generalization on unseen domains via inference-time label-preserving target projections. In *Computer Vision and Pattern Recognition*, pages 12924–12933, 2021.
- [36] Seulki Park, Jongin Lim, Younghun Jeon, and Jin Young Choi. Influence-balanced loss for imbalanced visual classification. In *International Conference on Computer Vision*, 2021.
- [37] Hanyu Peng, Mingming Sun, and Ping Li. Optimal transport for long-tailed recognition with learnable cost matrix. In *International Conference on Learning Representations*, 2022.
- [38] Zhen Qiu, Yifan Zhang, Hongbin Lin, Shuaicheng Niu, Yanxia Liu, Qing Du, and Mingkui Tan. Source-free domain adaptation via avatar prototype generation and adaptation. In *International Joint Conference on Artificial Intelligence*, 2021.
- [39] Saurabh Sharma, Ning Yu, Mario Fritz, and Bernt Schiele. Long-tailed recognition using class-balanced experts. In *German Conference on Pattern Recognition*, pages 86–100, 2020.

- [40] Yu Sun, Xiaolong Wang, Zhuang Liu, John Miller, Alexei Efros, and Moritz Hardt. Test-time training with self-supervision for generalization under distribution shifts. In *International Conference on Machine Learning*, 2020.
- [41] Jingru Tan, Changbao Wang, Buyu Li, Quanquan Li, Wanli Ouyang, Changqing Yin, and Junjie Yan. Equalization loss for long-tailed object recognition. In *Computer Vision and Pattern Recognition*, pages 11662–11671, 2020.
- [42] Kaihua Tang, Jianqiang Huang, and Hanwang Zhang. Long-tailed classification by keeping the good and removing the bad momentum causal effect. In *Advances in Neural Information Processing Systems*, volume 33, 2020.
- [43] Junjiao Tian, Yen-Cheng Liu, et al. Posterior re-calibration for imbalanced datasets. In *Advances in Neural Information Processing Systems*, 2020.
- [44] Grant Van Horn, Oisinand Mac Aodha, et al. The inaturalist species classification and detection dataset. In *Computer Vision and Pattern Recognition*, 2018.
- [45] Thomas Varsavsky, Mauricio Orbes-Arteaga, et al. Test-time unsupervised domain adaptation. In *International Conference on Medical Image Computing and Computer-Assisted Intervention*, pages 428–436, 2020.
- [46] Dequan Wang, Evan Shelhamer, Shaoteng Liu, Bruno Olshausen, and Trevor Darrell. Tent: Fully test-time adaptation by entropy minimization. In *International Conference on Learning Representations*, 2021.
- [47] Jiaqi Wang, Wenwei Zhang, Yuhang Zang, Yuhang Cao, Jiangmiao Pang, Tao Gong, Kai Chen, Ziwei Liu, Chen Change Loy, and Dahua Lin. Seesaw loss for long-tailed instance segmentation. In *Computer Vision and Pattern Recognition*, pages 9695–9704, 2021.
- [48] Peng Wang, Kai Han, et al. Contrastive learning based hybrid networks for long-tailed image classification. In *Computer Vision and Pattern Recognition*, 2021.
- [49] Xudong Wang, Long Lian, Zhongqi Miao, Ziwei Liu, and Stella X Yu. Long-tailed recognition by routing diverse distribution-aware experts. In *International Conference on Learning Representations*, 2021.
- [50] Yandong Wen, Kaipeng Zhang, et al. A discriminative feature learning approach for deep face recognition. In *European Conference on Computer Vision*, 2016.
- [51] Yeming Wen, Dustin Tran, and Jimmy Ba. Batchensemble: an alternative approach to efficient ensemble and lifelong learning. In *International Conference on Learning Representations*, 2020.
- [52] Zhenzhen Weng, Mehmet Giray Ogut, Shai Limonchik, and Serena Yeung. Unsupervised discovery of the long-tail in instance segmentation using hierarchical self-supervision. In *Computer Vision and Pattern Recognition*, 2021.
- [53] Liuyu Xiang, Guiguang Ding, and Jungong Han. Learning from multiple experts: Self-paced knowledge distillation for long-tailed classification. In *European Conference on Computer Vision*, 2020.
- [54] Jason Yosinski, Jeff Clune, Yoshua Bengio, and Hod Lipson. How transferable are features in deep neural networks? In *Advances in Neural Information Processing Systems*, volume 27, pages 3320–3328, 2014.
- [55] Yuhang Zang, Chen Huang, and Chen Change Loy. Fasa: Feature augmentation and sampling adaptation for long-tailed instance segmentation. In *International Conference on Computer Vision*, 2021.
- [56] Songyang Zhang, Zeming Li, Shipeng Yan, Xuming He, and Jian Sun. Distribution alignment: A unified framework for long-tail visual recognition. In *Computer Vision and Pattern Recognition*, pages 2361–2370, 2021.
- [57] Yifan Zhang, Bryan Hooi, Lanqing Hong, and Jiashi Feng. Unleashing the power of contrastive self-supervised visual models via contrast-regularized fine-tuning. In *Advances in Neural Information Processing Systems*, 2021.
- [58] Yifan Zhang, Bingyi Kang, Bryan Hooi, Shuicheng Yan, and Jiashi Feng. Deep long-tailed learning: A survey. *arXiv preprint arXiv:2110.04596*, 2021.

- [59] Yifan Zhang, Ying Wei, et al. Collaborative unsupervised domain adaptation for medical image diagnosis. *IEEE Transactions on Image Processing*, 2020.
- [60] Yifan Zhang, Peilin Zhao, Jiezhong Cao, Wenye Ma, Junzhou Huang, Qingyao Wu, and Minghui Tan. Online adaptive asymmetric active learning for budgeted imbalanced data. In *ACM SIGKDD International Conference on Knowledge Discovery & Data Mining*, pages 2768–2777, 2018.
- [61] Peilin Zhao, Yifan Zhang, Min Wu, Steven CH Hoi, Minghui Tan, and Junzhou Huang. Adaptive cost-sensitive online classification. *IEEE Transactions on Knowledge and Data Engineering*, 31(2):214–228, 2018.
- [62] Zhisheng Zhong, Jiequan Cui, Shu Liu, and Jiaya Jia. Improving calibration for long-tailed recognition. In *Computer Vision and Pattern Recognition*, 2021.
- [63] Boyan Zhou, Quan Cui, Xiu-Shen Wei, and Zhao-Min Chen. Bbn: Bilateral-branch network with cumulative learning for long-tailed visual recognition. In *Computer Vision and Pattern Recognition*, pages 9719–9728, 2020.

Checklist

1. For all authors...
 - (a) Do the main claims made in the abstract and introduction accurately reflect the paper’s contributions and scope? [Yes]
 - (b) Did you describe the limitations of your work? [Yes] Please refer to Appendix H.
 - (c) Did you discuss any potential negative societal impacts of your work? [N/A] This is a fundamental research that does not have particular negative social impacts.
 - (d) Have you read the ethics review guidelines and ensured that your paper conforms to them? [Yes]
2. If you are including theoretical results...
 - (a) Did you state the full set of assumptions of all theoretical results? [Yes]
 - (b) Did you include complete proofs of all theoretical results? [Yes] Please refer to Appendix A.
3. If you ran experiments...
 - (a) Did you include the code, data, and instructions needed to reproduce the main experimental results (either in the supplemental material or as a URL)? [Yes] Please refer to the supplemental material.
 - (b) Did you specify all the training details (e.g., data splits, hyperparameters, how they were chosen)? [Yes] Please refer to Section 5.1 and Appendix C.
 - (c) Did you report error bars (e.g., with respect to the random seed after running experiments multiple times)? [N/A] The common practice in long-tailed recognition does not report error bars, so we follow the previous papers and do not report them.
 - (d) Did you include the total amount of compute and the type of resources used (e.g., type of GPUs, internal cluster, or cloud provider)? [Yes] Please refer to Appendix C.3 for details on different datasets.
4. If you are using existing assets (e.g., code, data, models) or curating/releasing new assets...
 - (a) If your work uses existing assets, did you cite the creators? [Yes]
 - (b) Did you mention the license of the assets? [N/A] All the used benchmark datasets are publicly available.
 - (c) Did you include any new assets either in the supplemental material or as a URL? [Yes] We submitted the source codes of our method as an anonymized zip file.
 - (d) Did you discuss whether and how consent was obtained from people whose data you’re using/curating? [N/A] These datasets are open-source benchmark datasets.
 - (e) Did you discuss whether the data you are using/curating contains personally identifiable information or offensive content? [N/A] These datasets are open-source benchmark datasets.
5. If you used crowdsourcing or conducted research with human subjects...
 - (a) Did you include the full text of instructions given to participants and screenshots, if applicable? [N/A]
 - (b) Did you describe any potential participant risks, with links to Institutional Review Board (IRB) approvals, if applicable? [N/A]
 - (c) Did you include the estimated hourly wage paid to participants and the total amount spent on participant compensation? [N/A]

Supplementary Materials

We organize the supplementary materials as follows:

- Appendix A: the proofs for Theorem 1.
- Appendix B: the pseudo-code of the proposed method.
- Appendix C: more details of experimental settings.
- Appendix D: more empirical results on vanilla long-tailed recognition, test-agnostic long-tailed recognition, skill-diverse expert learning, and test-time self-supervised aggregation.
- Appendix E: more ablation studies on expert learning and the proposed inverse softmax loss.
- Appendix F: more ablation studies on test-time self-supervised aggregation.
- Appendix G: more discussion on model complexity.
- Appendix H: discussion on potential limitations.

A Proofs for Theorem 1

Proof. We first recall several key notations and define some new notations. The random variables of model predictions and ground-truth labels are defined as $\hat{Y} \sim p(\hat{y})$ and $Y \sim p(y)$, respectively. The number of classes is denoted by C . Moreover, we further denote the test sample set of the class k by \mathcal{Z}_k , in which the total number of samples in this class is denoted by $|\mathcal{Z}_k|$. Let $c_k = \frac{1}{|\mathcal{Z}_k|} \sum_{\hat{y} \in \mathcal{Z}_k} \hat{y}$ represent the hard mean of all predictions of samples from the class k , and let $\stackrel{c}{=}$ indicate equality up to a multiplicative and/or additive constant.

As shown in Eq.(4), the optimization objective of our test-time self-supervised aggregation method is to maximize $\mathcal{S} = \sum_{j=1}^{n_t} \hat{y}_j^1 \cdot \hat{y}_j^2$, where n_t denotes the number of test samples. For convenience, we simplify the first data view to be the original data, so the objective function becomes $\sum_{j=1}^{n_t} \hat{y}_j \cdot \hat{y}_j^1$. Maximizing such an objective is equivalent to minimizing $\sum_{j=1}^{n_t} -\hat{y}_j \cdot \hat{y}_j^1$. Here, we assume the data augmentations are strong enough to generate representative data views that can simulate the test data from the same class. In this sense, the new data view can be regarded as an independent sample from the same class. Following this, we analyze our method by connecting $-\hat{y}_j \cdot \hat{y}_j^1$ to $\sum_{\hat{y}_j \in \mathcal{Z}_k} \|\hat{y}_j - c_k\|^2$, which is similar to the tightness term in the center loss [50]:

$$\begin{aligned}
 \sum_{\hat{y}_j, \hat{y}_j^1 \in \mathcal{Z}_k} -\hat{y}_j \cdot \hat{y}_j^1 &\stackrel{c}{=} \frac{1}{|\mathcal{Z}_k|} \sum_{\hat{y}_j, \hat{y}_j^1 \in \mathcal{Z}_k} -\hat{y}_j \cdot \hat{y}_j^1 \stackrel{c}{=} \frac{1}{|\mathcal{Z}_k|} \sum_{\hat{y}_j, \hat{y}_j^1 \in \mathcal{Z}_k} \|\hat{y}_j\|^2 - \hat{y}_j \cdot \hat{y}_j^1 \\
 &= \sum_{\hat{y}_j \in \mathcal{Z}_k} \|\hat{y}_j\|^2 - \frac{1}{|\mathcal{Z}_k|} \sum_{\hat{y}_j \in \mathcal{Z}_k} \sum_{\hat{y}_j^1 \in \mathcal{Z}_k} \hat{y}_j \cdot \hat{y}_j^1 \\
 &= \sum_{\hat{y}_j \in \mathcal{Z}_k} \|\hat{y}_j\|^2 - 2 \frac{1}{|\mathcal{Z}_k|} \sum_{\hat{y}_j \in \mathcal{Z}_k} \sum_{\hat{y}_j^1 \in \mathcal{Z}_k} \hat{y}_j \cdot \hat{y}_j^1 + \frac{1}{|\mathcal{Z}_k|} \sum_{\hat{y}_j \in \mathcal{Z}_k} \sum_{\hat{y}_j^1 \in \mathcal{Z}_k} \hat{y}_j \cdot \hat{y}_j^1 \\
 &= \sum_{\hat{y}_j \in \mathcal{Z}_k} \|\hat{y}_j\|^2 - 2 \hat{y}_j \cdot c_k + \|c_k\|^2 \\
 &= \sum_{\hat{y}_j \in \mathcal{Z}_k} \|\hat{y}_j - c_k\|^2,
 \end{aligned}$$

where we use the property of the normalized predictions, *i.e.*, $\|\hat{y}_j\|^2 = \|\hat{y}_j^1\|^2 = 1$, and the definition of the class hard mean $c_k = \frac{1}{|\mathcal{Z}_k|} \sum_{\hat{y} \in \mathcal{Z}_k} \hat{y}$.

By summing over all classes k , we obtain:

$$\sum_{j=1}^{n_t} -\hat{y}_j \cdot \hat{y}_j^1 \stackrel{c}{=} \sum_{j=1}^{n_t} \|\hat{y}_j - c_{y_i}\|^2.$$

Based on this equation, following [1, 57], we can interpret $\sum_{j=1}^{n_t} -\hat{y}_j \cdot \hat{y}_j^1$ as a conditional cross-entropy between \hat{Y} and another random variable \bar{Y} , whose conditional distribution given Y is a standard Gaussian centered around $c_Y: \bar{Y} | Y \sim \mathcal{N}(c_Y, i)$:

$$\sum_{j=1}^{n_t} -\hat{y}_j \cdot \hat{y}_j^1 \stackrel{c}{=} \mathcal{H}(\hat{Y}; \bar{Y} | Y) = \mathcal{H}(\hat{Y} | Y) + \mathcal{D}_{KL}(\hat{Y} || \bar{Y} | Y).$$

Hence, we know that $\sum_{j=1}^{n_t} -\hat{y}_j \cdot \hat{y}_j^1$ is an upper bound on the conditional entropy of predictions \hat{Y} given labels Y :

$$\sum_{j=1}^{n_t} -\hat{y}_j \cdot \hat{y}_j^1 \stackrel{c}{\geq} \mathcal{H}(\hat{Y} | Y),$$

where the symbol $\stackrel{c}{\geq}$ represents “larger than” up to a multiplicative and/or an additive constant. Moreover, when $\hat{Y} | Y \sim \mathcal{N}(c_Y, i)$, the bound is tight. As a result, minimizing $\sum_{j=1}^{n_t} -\hat{y}_j \cdot \hat{y}_j^1$ is equivalent to minimizing $\mathcal{H}(\hat{Y} | Y)$:

$$\sum_{j=1}^{n_t} -\hat{y}_j \cdot \hat{y}_j^1 \propto \mathcal{H}(\hat{Y} | Y). \quad (5)$$

Meanwhile, the mutual information between predictions \hat{Y} and labels Y can be represented by:

$$\mathcal{I}(\hat{Y}; Y) = \mathcal{H}(\hat{Y}) - \mathcal{H}(\hat{Y} | Y). \quad (6)$$

Combining Eqs.(5-6), we have:

$$\sum_{j=1}^{n_t} -\hat{y}_j \cdot \hat{y}_j^1 \propto -\mathcal{I}(\hat{Y}; Y) + \mathcal{H}(\hat{Y}).$$

Since $\mathcal{S} = \sum_{j=1}^{n_t} \hat{y}_j \cdot \hat{y}_j^1$, we obtain:

$$\mathcal{S} \propto \mathcal{I}(\hat{Y}; Y) - \mathcal{H}(\hat{Y}),$$

which concludes the proof for Theorem 1. \square

B Pseudo-code

This appendix provides the pseudo-code¹ of SADE, which consists of skill-diverse expert learning and test-time self-supervised aggregation. Here, the skill-diverse expert learning strategy is summarized in Algorithm 1. For simplicity, we depict the pseudo-code based on batch size 1, but we conduct batch gradient descent in practice.

Algorithm 1 Skill-diverse Expert Learning

Require: Epochs T ; Hyper-parameters λ for \mathcal{L}_{inv}

Initialize: Network backbone f_θ ; Experts E_1, E_2, E_3

```

1: for  $e=1, \dots, T$  do
2:   for  $x \in \mathcal{D}_s$  do // batch sampling in practice
3:     Obtain logits  $v_1$  based on  $f_\theta$  and  $E_1$ ;
4:     Obtain logits  $v_2$  based on  $f_\theta$  and  $E_2$ ;
5:     Obtain logits  $v_3$  based on  $f_\theta$  and  $E_3$ ;
6:     Compute loss  $\mathcal{L}_{ce}$  with  $v_1$  for Expert  $E_1$ ; // Eq.(1)
7:     Compute loss  $\mathcal{L}_{bal}$  with  $v_2$  for Expert  $E_2$ ; // Eq.(2)
8:     Compute loss  $\mathcal{L}_{inv}$  with  $v_3$  for Expert  $E_3$ ; // Eq.(3)
9:     Train the model with  $\mathcal{L}_{ce} + \mathcal{L}_{bal} + \mathcal{L}_{inv}$ .
10:  end for
11: end for
Output: The trained model  $\{f_\theta, E_1, E_2, E_3\}$ 

```

After training the multiple skill-diverse experts with Algorithm 1, the final prediction of the multi-expert model for vanilla long-tailed recognition is the arithmetic mean of the prediction logits of these experts, followed by a softmax function.

When it comes to test-agnostic long-tailed recognition, we need to aggregate these skill-diverse experts to handle the unknown test class distribution based on Algorithm 2. Here, to avoid the learned weights of some weak experts becoming zero, we give a stopping condition in Algorithm 2: if the weight for one expert is less than 0.05, we stop test-time training. Retaining a small amount of weight for each expert is sufficient to ensure the effect of ensemble learning.

Algorithm 2 Test-time Self-supervised Aggregation

Require: Epochs T' ; The trained backbone f_θ ; The trained experts E_1, E_2, E_3

Initialize: Expert aggregation weights w // uniform initialization

```

1: for  $e=1, \dots, T'$  do
2:   for  $x \in \mathcal{D}_t$  do // batch sampling in practice
3:     Draw two data augmentation functions  $t \sim \mathcal{T}, t' \sim \mathcal{T}$ ;
4:     Generate data views  $x^1=t(x), x^2=t'(x)$ ;
5:     Obtain logits  $v_1^1, v_2^1, v_3^1$  for the view  $x^1$ ;
6:     Obtain logits  $v_1^2, v_2^2, v_3^2$  for the view  $x^2$ ;
7:     Normalize expert weights  $w$  via softmax function;
8:     Conduct predictions  $\hat{y}^1, \hat{y}^2$  based on  $\hat{y}=wv$ ;
9:     Compute prediction stability  $\mathcal{S}$ ; // Eq. (4)
10:    Maximize  $\mathcal{S}$  to update  $w$ ;
11:  end for
12:  If  $w_i \leq 0.05$  for any  $w_i \in w$ , then stop training.
13: end for
Output: Expert aggregation weights  $w$ 

```

Note that, in test-agnostic long-tailed recognition, each model is only trained once on long-tailed training data and then directly evaluated on multiple test sets. Our test-time self-supervised strategy adapts the trained multi-expert model using only unlabeled test data during testing.

¹The source code is provided in the supplementary material.

C More Experimental Settings

In this appendix, we provide more details on experimental settings.

C.1 Benchmark Datasets

We use four benchmark datasets (*i.e.*, ImageNet-LT [31], CIFAR100-LT [3], Places-LT [31], and iNaturalist 2018 [44]) to simulate real-world long-tailed class distributions. These datasets suffer from severe class imbalance [22, 60]. Their data statistics are summarized in Table 11, where CIFAR100-LT has three variants with different imbalance ratios. The imbalance ratio is defined as $\max n_j / \min n_j$, where n_j denotes the data number of class j .

Table 11: Statistics of datasets.

Dataset	# classes	# training data	# test data	imbalance ratio
ImageNet-LT [31]	1,000	115,846	50,000	256
CIFAR100-LT [3]	100	50,000	10,000	{10,50,100}
Places-LT [31]	365	62,500	36,500	996
iNaturalist 2018 [44]	8,142	437,513	24,426	500

C.2 Construction of Test-agnostic Long-tailed Datasets

Following LADE [17], we construct three kinds of test class distributions, *i.e.*, the uniform distribution, forward long-tailed distributions and backward long-tailed distributions. In the backward ones, the long-tailed class order is flipped. Here, the forward and backward long-tailed test distributions contain multiple different imbalance ratios, *i.e.*, $\rho \in \{2, 5, 10, 25, 50\}$. Note that LADE [17] only constructed multiple distribution-agnostic test datasets for ImageNet-LT; while in this study, we use the same way to construct distribution-agnostic test datasets for the remaining benchmark datasets, *i.e.*, CIFAR100-LT, Places-LT and iNaturalist 2018, as illustrated below.

Considering the long-tailed training classes are sorted in a decreasing order, the various test datasets are constructed as follows: (1) Forward long-tailed distribution: the number of the j -th class is $n_j = N \cdot \rho^{(j-1)/C}$, where N indicates the sample number per class in the original uniform test dataset and C is the number of classes. (2) Backward long-tailed distribution: the number of the j -th class is $n_j = N \cdot \rho^{(C-j)/C}$. In the backward long-tailed distributions, the order of the long tail on classes is flipped, so the distribution shift between training and test data is large, especially when the imbalance ratio gets higher.

For ImageNet-LT, CIFAR100-LT and Places-LT, since there are enough test samples per class, we follow the setting in LADE [17] and construct the imbalance ratio set by $\rho \in \{2, 5, 10, 25, 50\}$. For iNaturalist 2018, since each class only contains three test samples, we adjust the imbalance ratio set to $\rho \in \{2, 3\}$. Note that when we set $\rho = 3$, there are some classes in iNaturalist 2018 containing no test sample. All these constructed distribution-agnostic long-tailed datasets will be publicly available along with our code.

C.3 More Implementation Details of Our Method

We implement our method in PyTorch. Following [17, 49], we use ResNeXt-50 for ImageNet-LT, ResNet-32 for CIFAR100-LT, ResNet-152 for Places-LT and ResNet-50 for iNaturalist 2018 as backbones, respectively. Moreover, we adopt the cosine classifier for prediction on all datasets.

Although we have depicted the skill-diverse multi-expert framework in Section 4.1, we give more details about it here. Without loss of generality, we take ResNet [15] as an example to illustrate the multi-expert model. Since the shallow layers extract more general features and deeper layers extract more task-specific features [54], the three-expert model uses the first two stages of ResNet as the expert-shared backbone, while the later stages of ResNet and the fully-connected layer constitute independent components of each expert. To be more specific, the number of convolutional filters in each expert is reduced by 1/4, since by sharing the backbone and using fewer filters in each expert [49, 63], the computational complexity of the model is reduced compared to the model with independent experts. The final prediction is the arithmetic mean of the prediction logits of these experts, followed by a softmax function.

In the training phase, the data augmentations are the same as previous long-tailed studies [17, 25]. If not specified, we use the SGD optimizer with the momentum of 0.9 and set the initial learning rate as 0.1 with linear decay. More specifically, for ImageNet-LT, we train models for 180 epochs with batch size 64 and a learning rate of 0.025 (cosine decay). For CIFAR100-LT, the training epoch is 200 and the batch size is 128. For Places-LT, following [31], we use ImageNet pre-trained ResNet-152 as the backbone, while the batch size is set to 128 and the training epoch is 30. Besides, the learning rate is 0.01 for the classifier and 0.001 for all other layers. For iNaturalist 2018, we set the training epoch to 200, the batch size to 512 and the learning rate to 0.2. In our inverse softmax loss, we set $\lambda=2$ for ImageNet-LT and CIFAR100-LT, and $\lambda=1$ for the remaining datasets.

In the test-time training, we use the same augmentations as MoCo v2 [5] to generate different data views, *i.e.*, random resized crop, color jitter, gray scale, Gaussian blur and horizontal flip. If not specified, we train the aggregation weights for 5 epochs with the batch size 128, where we adopt the same optimizer and learning rate as the training phase.

More detailed statistics of network architectures and hyper-parameters are reported in Table 12. Based on these hyper-parameters, we conduct experiments on 1 TITAN RTX 2080 GPU for CIFAR100-LT, 4 GPUs for iNaturalist18, and 2 GPUs for ImageNet-LT and Places-LT, respectively. The source code of our method is available in the supplementary material.

Table 12: Statistics of the used network architectures and hyper-parameters in our study.

Items	ImageNet-LT	CIFAR100LT	Places-LT	iNarutalist 2018
Network Architectures				
network backbone	ResNeXt-50	ResNet-32	ResNet-152	ResNet-50
classifier	cosine classifier			
Training Phase				
epochs	180	200	30	200
batch size	64	128	128	512
learning rate (lr)	0.025	0.1	0.01	0.2
lr schedule	cosine decay	linear decay		
λ in inverse softmax loss	2		1	
weight decay factor	5×10^{-4}	5×10^{-4}	4×10^{-4}	2×10^{-4}
momentum factor	0.9			
optimizer	SGD optimizer with nesterov			
Test-time Training				
epochs	5			
batch size	128			
learning rate (lr)	0.025	0.1	0.01	0.1

C.4 Discussions on Evaluation Metric

As mentioned in Section 5.1, we follow LADE [17] and use micro accuracy to evaluate model performance on test-agnostic long-tailed recognition. In this appendix, we explain why micro accuracy is a better metric than macro accuracy when the test dataset exhibits a non-uniform class distribution. For instance, in the test scenario with a backward long-tailed class distribution, the tail classes are more frequently encountered than the head classes, and thus should have larger weights in evaluation. However, simply using macro accuracy treats all the categories equally and cannot differentiate classes of different frequencies.

For example, one may train a recognition model for autonomous cars based on the training data collected from city areas, where pedestrians are majority classes and stone obstacles are minority classes. Assume the model accuracy is 60% on pedestrians and 40% on stones. If deploying the model to city areas, where pedestrians/stones are assumed to have 500/50 test data, then the macro accuracy is 50% and the micro accuracy is $\frac{500 \times 0.6 + 50 \times 0.4}{500 + 50} \approx 58\%$. In contrast, when deploying the model to mountain areas, the pedestrians become the minority, while stones become the majority. Assuming the test data numbers are changed to 50/500 on pedestrians/stones, the micro accuracy is adjusted to $\frac{50 \times 0.6 + 500 \times 0.4}{50 + 500} \approx 42\%$, but the macro accuracy is still 50%. In this case, macro accuracy is less informative than micro accuracy for measuring model performance. Therefore, micro accuracy is a better metric to evaluate the performance of test-agnostic long-tailed recognition.

D More Empirical Results

D.1 More Results on Vanilla Long-tailed Recognition

Accuracy on class subsets In the main paper, we have provided the average performance over all classes on the uniform test class distribution. In this appendix, we further report the accuracy regarding various class subsets (c.f. Table 13), making the results more complete.

Table 13: Top-1 accuracy of long-tailed recognition methods on the uniform test distribution.

Method	ImageNet-LT				CIFAR100-LT(IR10)				CIFAR100-LT(IR50)			
	Many	Med.	Few	All	Many	Med.	Few	All	Many	Med.	Few	All
Softmax	68.1	41.5	14.0	48.0	66.0	42.7	-	59.1	66.8	37.4	15.5	45.6
Causal [42]	64.1	45.8	27.2	50.3	63.3	49.9	-	59.4	62.9	44.9	26.2	48.8
Balanced Softmax [21]	64.1	48.2	33.4	52.3	63.4	55.7	-	61.0	62.1	45.6	36.7	50.9
MiSLAS [62]	62.0	49.1	32.8	51.4	64.9	56.6	-	62.5	61.8	48.9	33.9	51.5
LADE [17]	64.4	47.7	34.3	52.3	63.8	56.0	-	61.6	60.2	46.2	35.6	50.1
RIDE [49]	68.0	52.9	35.1	56.3	65.7	53.3	-	61.8	66.6	46.2	30.3	51.7
SADE (ours)	66.5	57.0	43.5	58.8	65.8	58.8	-	63.6	61.5	50.2	45.0	53.9

Method	CIFAR100-LT(IR100)				Places-LT				iNaturalist 2018			
	Many	Med.	Few	All	Many	Med.	Few	All	Many	Med.	Few	All
Softmax	68.6	41.1	9.6	41.4	46.2	27.5	12.7	31.4	74.7	66.3	60.0	64.7
Causal [42]	64.1	46.8	19.9	45.0	23.8	35.7	39.8	32.2	71.0	66.7	59.7	64.4
Balanced Softmax [21]	59.5	45.4	30.7	46.1	42.6	39.8	32.7	39.4	70.9	70.7	70.4	70.6
MiSLAS [62]	60.4	49.6	26.6	46.8	41.6	39.3	27.5	37.6	71.7	71.5	69.7	70.7
LADE [17]	58.7	45.8	29.8	45.6	42.6	39.4	32.3	39.2	68.9	68.7	70.2	69.3
RIDE [49]	67.4	49.5	23.7	48.0	43.1	41.0	33.0	40.3	71.5	70.0	71.6	71.8
SADE (ours)	65.4	49.3	29.3	49.8	40.4	43.2	36.8	40.9	74.5	72.5	73.0	72.9

Results on stronger data augmentations Inspired by PaCo [8], we further evaluate SADE training with stronger data augmentation (*i.e.*, RandAugment [7]) for 400 epochs. The results in Table 14 further demonstrate the state-of-the-art performance of SADE.

Table 14: Accuracy of long-tailed methods with stronger augmentations, where the test class distribution is uniform. Here, * denotes training with RandAugment [7] for 400 epochs. The baseline results are directly copied from the work [8].

Methods	ImageNet-LT	CIFAR100-LT(IR10)	CIFAR100-LT(IR50)	CIFAR100-LT(IR100)	Places-LT	iNaturalist 2018
PaCo* [8]	58.2	64.2	56.0	52.0	41.2	73.2
SADE* (ours)	61.2	65.3	57.3	52.2	41.3	74.5

Results on more neural architectures In addition to using the common practice of backbones as previous long-tailed studies [17, 49], we further evaluate SADE on more neural architectures. The results in Table 15 demonstrate that SADE is able to train different network backbones well.

Table 15: Accuracy of SADE with various network architectures. Here, * denotes training with RandAugment [7] for 400 epochs.

ImageNet-LT						iNaturalist 2018					
Backbone	Methods	Many	Med.	Few	All	Backbone	Methods	Many	Med.	Few	All
ResNeXt-50	SADE	66.5	57.0	43.5	58.8	ResNet-50	SADE	74.5	72.5	73.0	72.9
	SADE*	67.3	60.4	46.4	61.2		SADE*	75.5	73.7	75.1	74.5
ResNeXt-101	SADE	66.8	57.5	43.1	59.1	ResNet-152	SADE	76.2	64.3	65.1	74.8
	SADE*	68.1	60.5	45.5	61.4		SADE*	78.3	77.0	76.7	77.0
ResNeXt-152	SADE	67.2	57.4	43.5	59.3						
	SADE*	68.6	61.2	47.0	62.1						

Results on more datasets We also conduct experiments on CIFAR10-LT with imbalance ratios of 10 and 100. Promising results in Table 16 further demonstrate the effectiveness and superiority of our proposed method.

Table 16: Accuracy on CIFAR10-LT, where the test class distribution is uniform. Most results are directly copied from the work [62].

Imbalance Ratio	Softmax	BBN	MiSLAS	RIDE	SADE (ours)
10	86.4	88.4	90.0	89.7	90.8
100	70.4	79.9	82.1	81.6	83.8

D.2 More Results on Test-agnostic Long-tailed Recognition

In the main paper, we have provided the overall performance on four benchmark datasets with various test class distributions (cf. Table 5). In this appendix, we further verify the effectiveness of our method on more dataset settings (*i.e.*, CIFAR100-IR10 and CIFAR100-IR50), as shown in Table 17.

Table 17: Top-1 accuracy over all classes on various unknown test class distributions. “Prior” indicates that the test class distribution is used as prior knowledge. “Uni.” denotes the uniform distribution. “IR” indicates the imbalance ratio. “BS” denotes the balanced softmax [21].

(a) ImageNet-LT												(b) CIFAR100-LT (IR10)																							
Method	Prior	Forward-LT					Uni.	Backward-LT					Forward-LT					Uni.	Backward-LT																
		50	25	10	5	2	1	2	5	10	25	50	50	25	10	5	2	1	2	5	10	25	50												
Softmax	✗	66.1	63.8	60.3	56.6	52.0	48.0	43.9	38.6	34.9	30.9	27.6	72.0	69.6	66.4	65.0	61.2	59.1	56.3	53.5	50.5	48.7	46.5												
BS	✗	63.2	61.9	59.5	57.2	54.4	52.3	50.0	47.0	45.0	42.3	40.8	65.9	64.9	64.1	63.4	61.8	61.0	60.0	58.2	57.5	56.2	55.1												
MiSLAS	✗	61.6	60.4	58.0	56.3	53.7	51.4	49.2	46.1	44.0	41.5	39.5	67.0	66.1	65.5	64.4	63.2	62.5	61.2	60.4	59.3	58.5	57.7												
LADE	✗	63.4	62.1	59.9	57.4	54.6	52.3	49.9	46.8	44.9	42.7	40.7	67.5	65.8	65.8	64.4	62.7	61.6	60.5	58.8	58.3	57.4	57.7												
LADE	✓	65.8	63.8	60.6	57.5	54.5	52.3	50.4	48.8	48.6	49.0	49.2	71.2	69.3	67.1	64.6	62.4	61.6	60.4	61.4	61.5	62.7	64.8												
RIDE	✗	67.6	66.3	64.0	61.7	58.9	56.3	54.0	51.0	48.7	46.2	44.0	67.1	65.3	63.6	62.1	60.9	61.8	58.4	56.8	55.3	54.9	53.4												
SADE	✗	69.4	67.4	65.4	63.0	60.6	58.8	57.1	55.5	54.5	53.7	53.1	71.2	69.4	67.6	66.3	64.4	63.6	62.9	62.4	61.7	62.1	63.0												
(c) CIFAR100-LT (IR50)																								(d) CIFAR100-LT (IR100)											
Method	Prior	Forward-LT					Uni.	Backward-LT					Forward-LT					Uni.	Backward-LT																
		50	25	10	5	2	1	2	5	10	25	50	50	25	10	5	2	1	2	5	10	25	50												
Softmax	✗	64.8	62.7	58.5	55.0	49.9	45.6	40.9	36.2	32.1	26.6	24.6	63.3	62.0	56.2	52.5	46.4	41.4	36.5	30.5	25.8	21.7	17.5												
BS	✗	61.6	60.2	58.4	55.9	53.7	50.9	48.5	45.7	43.9	42.5	40.6	57.8	55.5	54.2	52.0	48.7	46.1	43.6	40.8	38.4	36.3	33.7												
MiSLAS	✗	60.1	58.9	57.7	56.2	53.7	51.5	48.7	46.5	44.3	41.8	40.2	58.8	57.2	55.2	53.0	49.6	46.8	43.6	40.1	37.7	33.9	32.1												
LADE	✗	61.3	60.2	56.9	54.3	52.3	50.1	47.8	45.7	44.0	41.8	40.5	56.0	55.5	52.8	51.0	48.0	45.6	43.2	40.0	38.3	35.5	34.0												
LADE	✓	65.9	62.1	58.8	56.0	52.3	50.1	48.3	45.5	46.5	46.8	47.8	62.6	60.2	55.6	52.7	48.2	45.6	43.8	41.1	41.5	40.7	41.6												
RIDE	✗	62.2	61.0	58.8	56.4	52.9	51.7	47.1	44.0	41.4	38.7	37.1	63.0	59.9	57.0	53.6	49.4	48.0	42.5	38.1	35.4	31.6	29.2												
SADE	✗	67.2	64.5	61.2	58.6	55.4	53.9	51.9	50.9	51.0	51.7	52.8	65.9	62.5	58.3	54.8	51.1	49.8	46.2	44.7	43.9	42.5	42.4												
(e) Places-LT												(f) iNaturalist 2018																							
Method	Prior	Forward-LT					Uni.	Backward-LT					Forward-LT		Uni.	Backward-LT																			
		50	25	10	5	2	1	2	5	10	25	50	3	2	1	2	3																		
Softmax	✗	45.6	42.7	40.2	38.0	34.1	31.4	28.4	25.4	23.4	20.8	19.4	65.4	65.5	64.7	64.0	63.4																		
BS	✗	42.7	41.7	41.3	41.0	40.0	39.4	38.5	37.8	37.1	36.2	35.6	70.3	70.5	70.6	70.6	70.6																		
MiSLAS	✗	40.9	39.7	39.5	39.6	38.8	38.3	37.3	36.7	35.8	34.7	34.4	70.8	70.8	70.7	70.7	70.2																		
LADE	✗	42.8	41.5	41.2	40.8	39.8	39.2	38.1	37.6	36.9	36.0	35.7	68.4	69.0	69.3	69.6	69.5																		
LADE	✓	46.3	44.2	42.2	41.2	39.7	39.4	39.2	39.9	40.9	42.4	43.0	✗	69.1	69.3	70.2	✗																		
RIDE	✗	43.1	41.8	41.6	42.0	41.0	40.3	39.6	38.7	38.2	37.0	36.9	71.5	71.9	71.8	71.8	71.8																		
SADE	✗	46.4	44.9	43.3	42.6	41.3	40.9	40.6	41.1	41.4	42.0	41.6	72.3	72.5	72.9	73.5	73.3																		

Furthermore, we plot the results of all methods under these benchmark datasets with various test class distributions in Figure 4. To be specific, Softmax only performs well on highly-imbalanced forward long-tailed class distributions. Existing long-tailed baselines outperform Softmax, but they cannot handle backward test class distributions well. In contrast, our method consistently outperforms baselines on all benchmark datasets, particularly on the backward long-tailed test distributions with a relatively large imbalance ratio.

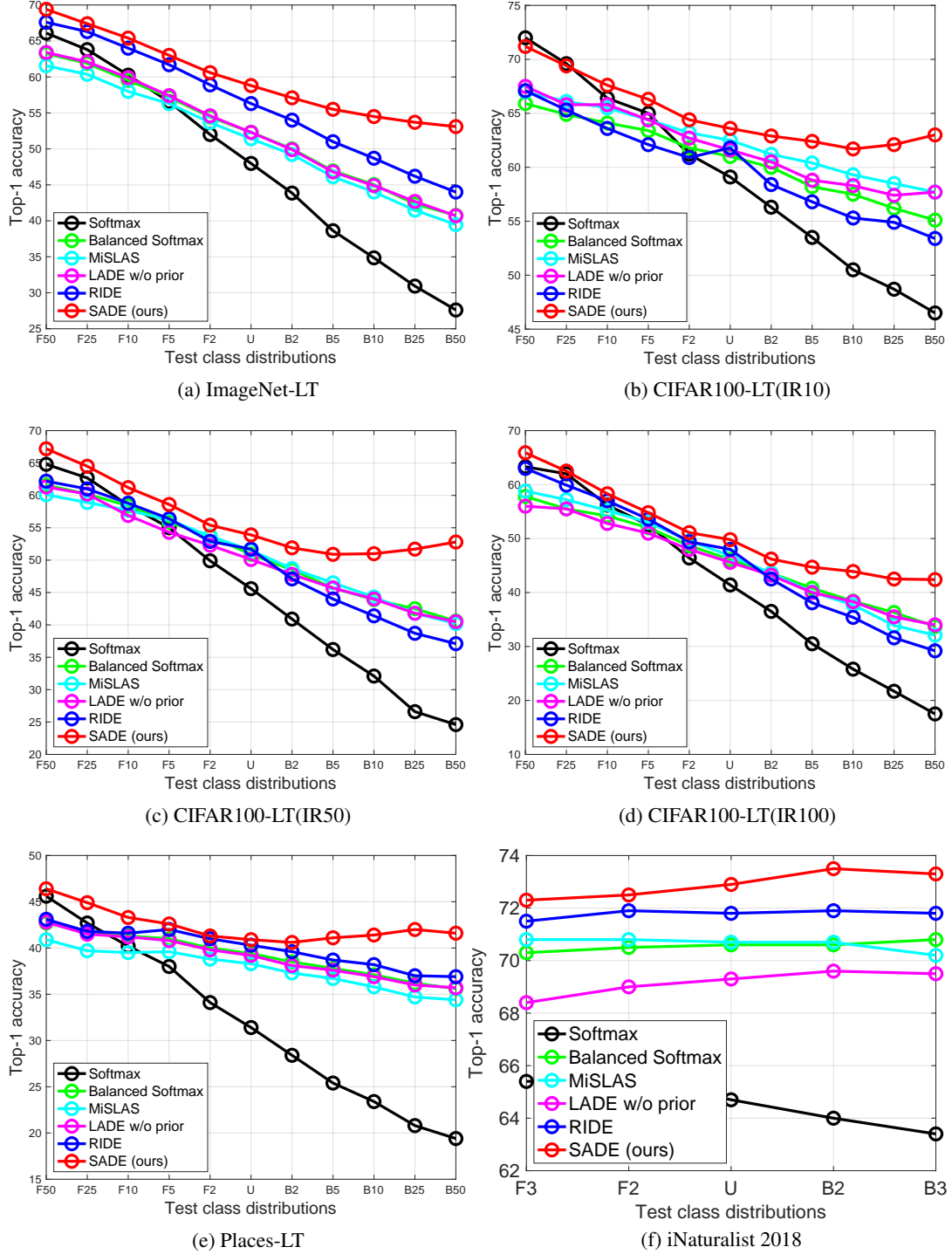


Figure 4: Performance visualizations on various unknown test class distributions, where “F” indicates the forward long-tailed distributions as training data, “B” indicates the backward long-tailed distributions to the training data, and “U” denotes the uniform distribution.

D.3 More Results on Skill-diverse Expert Learning

This appendix further evaluates the skill-diverse expert learning strategy on CIFAR100-LT, Places-LT and iNaturalist 2018 datasets. We report the results in Table 18, from which we draw the following observations. RIDE [49] is one of the state-of-the-art ensemble-based long-tailed methods, which tries to learn diverse distribution-aware experts by maximizing the divergence among expert predictions. However, such a method cannot learn sufficiently diverse experts. As shown in Table 18, the three experts in RIDE perform very similarly on various groups of classes under all benchmark datasets, and each expert has similar overall performance on each dataset. Such results demonstrate that simply maximizing the KL divergence of different experts’ predictions is not sufficient to learn visibly diverse distribution-aware experts.

In contrast, our proposed method learns the skill-diverse experts by directly training each expert with their customized expertise-guided objective functions, respectively. To be specific, the forward expert E_1 seeks to learn the long-tailed training distribution, so we directly train it with the cross-entropy loss. For the uniform expert E_2 , we use the balanced softmax loss to simulate the uniform test distribution. For the backward expert E_3 , we design a novel inverse softmax loss to train the expert, so that it simulates the inversely long-tailed class distribution. Table 18 shows that the three experts trained by our method are visibly diverse and skilled in handling different class distributions. Specifically, the forward expert is skilled in many-shot classes, the uniform expert is more balanced with higher overall performance, and the backward expert is good at few-shot classes. Because of such a novel design that enhances expert diversity, our method achieves more promising ensemble performance compared to RIDE.

Table 18: Performance of each expert on the uniform test distribution. Here, the training imbalance ratio of CIFAR100-LT is 100. The results show that our proposed method learns more skill-diverse experts, leading to better performance of ensemble aggregation.

Model	RIDE [49]															
	ImageNet-LT				CIFAR100-LT				Places-LT				iNaturalist 2018			
	Many	Med.	Few	All	Many	Med.	Few	All	Many	Med.	Few	All	Many	Med.	Few	All
Expert E_1	64.3	49.0	31.9	52.6	63.5	44.8	20.3	44.0	41.3	40.8	33.2	40.1	66.6	67.1	66.5	66.8
Expert E_2	64.7	49.4	31.2	52.8	63.1	44.7	20.2	43.8	43.0	40.9	33.6	40.3	66.1	67.1	66.6	66.8
Expert E_3	64.3	48.9	31.8	52.5	63.9	45.1	20.5	44.3	42.8	41.0	33.5	40.2	65.3	67.3	66.5	66.7
Ensemble	68.0	52.9	35.1	56.3	67.4	49.5	23.7	48.0	43.2	41.1	33.5	40.3	71.5	72.0	71.6	71.8

Model	SADE (ours)															
	ImageNet-LT				CIFAR100-LT				Places-LT				iNaturalist 2018			
	Many	Med.	Few	All	Many	Med.	Few	All	Many	Med.	Few	All	Many	Med.	Few	All
Expert E_1	68.8	43.7	17.2	49.8	67.6	36.3	6.8	38.4	47.6	27.1	10.3	31.2	76.0	67.1	59.3	66.0
Expert E_2	65.5	50.5	33.3	53.9	61.2	44.7	23.5	44.2	42.6	42.3	32.3	40.5	69.2	70.7	69.8	70.2
Expert E_3	43.4	48.6	53.9	47.3	14.0	27.6	41.2	25.8	22.6	37.2	45.6	33.6	55.6	61.5	72.1	65.1
Ensemble	67.0	56.7	42.6	58.8	61.6	50.5	33.9	49.4	40.4	43.2	36.8	40.9	74.4	72.5	73.1	72.9

D.4 More Results on Test-time Self-supervised Aggregation

This appendix provides more results to examine the effectiveness of our test-time self-supervised aggregation strategy. We report results in Table 19, from which we draw several observations.

First of all, our method is able to learn suitable expert aggregation weights for test-agnostic class distributions, without relying on the true test class distribution. For the forward long-tailed test distribution, where the test data number of many-shot classes is more than that of medium-shot and few-shot classes, our method learns a higher weight for the forward expert E_1 who is skilled in many-shot classes, and learns relatively low weights for the expert E_2 and expert E_3 who are good at medium-shot and few-shot classes. Meanwhile, for the uniform test class distribution where all classes have the same number of test samples, our test-time expert aggregation strategy learns relatively balanced weights for the three experts. For example, on the uniform ImageNet-LT test data, the learned weights by our strategy are 0.33, 0.33 and 0.34 for the three experts, respectively. In addition, for the backward long-tailed test distributions, our method learns a higher weight for the backward expert E_3 and a relatively low weight for the forward expert E_1 . Note that when the class imbalance ratio becomes larger, our method is able to learn more diverse expert weights adaptively for fitting the actual test class distributions.

Such results not only demonstrate the effectiveness of our proposed strategy, but also verify the theoretical analysis that our method can simulate the unknown test class distribution. To our best knowledge, such an ability is quite promising, since it is difficult to know the true test class distributions in real-world application. Therefore, our method opens the opportunity for tackling unknown class distribution shifts at test time, and can serve as a better candidate to handle real-world long-tailed learning applications.

Table 19: The learned aggregation weights by our test-time self-supervised aggregation strategy on different test class distributions of ImageNet-LT, CIFAR100-LT, Places-LT and iNaturalist 2018. The results show that our self-supervised strategy is able to learn suitable expert weights for various unknown test class distributions.

Test Dist.	ImageNet-LT			CIFAR100-LT(IR10)			CIFAR100-LT(IR50)		
	E1 (w_1)	E2 (w_2)	E3 (w_3)	E1 (w_1)	E2 (w_2)	E3 (w_3)	E1 (w_1)	E2 (w_2)	E3 (w_3)
Forward-LT-50	0.52	0.35	0.13	0.53	0.38	0.09	0.55	0.38	0.07
Forward-LT-25	0.50	0.35	0.15	0.52	0.37	0.11	0.54	0.38	0.08
Forward-LT-10	0.46	0.36	0.18	0.47	0.36	0.17	0.52	0.37	0.11
Forward-LT-5	0.43	0.34	0.23	0.46	0.34	0.20	0.50	0.36	0.14
Forward-LT-2	0.37	0.35	0.28	0.39	0.37	0.24	0.39	0.38	0.23
Uniform	0.33	0.33	0.34	0.38	0.32	0.3	0.35	0.33	0.33
Backward-LT-2	0.29	0.31	0.40	0.35	0.33	0.31	0.30	0.30	0.40
Backward-LT-5	0.24	0.31	0.45	0.31	0.32	0.37	0.21	0.29	0.50
Backward-LT-10	0.21	0.29	0.50	0.26	0.32	0.42	0.20	0.29	0.51
Backward-LT-25	0.18	0.29	0.53	0.24	0.30	0.46	0.18	0.27	0.55
Backward-LT-50	0.17	0.27	0.56	0.23	0.28	0.49	0.14	0.24	0.62

Test Dist.	CIFAR100-LT(IR100)			Places-LT			iNaturalist 2018		
	E1 (w_1)	E2 (w_2)	E3 (w_3)	E1 (w_1)	E2 (w_2)	E3 (w_3)	E1 (w_1)	E2 (w_2)	E3 (w_3)
Forward-LT-50	0.56	0.38	0.06	0.50	0.20	0.20	-	-	-
Forward-LT-25	0.55	0.38	0.07	0.50	0.20	0.20	-	-	-
Forward-LT-10	0.52	0.39	0.09	0.50	0.20	0.20	-	-	-
Forward-LT-5	0.51	0.37	0.12	0.46	0.32	0.22	-	-	-
Forward-LT-2	0.49	0.35	0.16	0.40	0.34	0.26	0.41	0.34	0.25
Uniform	0.40	0.35	0.24	0.25	0.34	0.41	0.33	0.33	0.34
Backward-LT-2	0.33	0.31	0.36	0.18	0.30	0.52	0.28	0.32	0.40
Backward-LT-5	0.28	0.30	0.42	0.17	0.28	0.55	-	-	-
Backward-LT-10	0.23	0.28	0.49	0.17	0.27	0.56	-	-	-
Backward-LT-25	0.21	0.26	0.53	0.17	0.27	0.56	-	-	-
Backward-LT-50	0.16	0.28	0.56	0.17	0.27	0.56	-	-	-

Relying on the learned expert weights, our method aggregates the three experts appropriately and achieves better performance on the dominant test classes, thus obtaining promising performance gains on various test distributions, as shown in Table 20. Note that the performance gain compared to existing methods gets larger as the test dataset gets more imbalanced. For example, on CIFAR100-LT with the imbalance ratio of 50, our test-time self-supervised strategy obtains a 7.7% performance gain on the Forward-LT-50 distribution and obtains a 9.2% performance gain on the Backward-LT-50 distribution, both of which are non-trivial. Such an observation is also supported by the visualization result of Figure 5, which plots the results of existing methods on ImageNet-LT with different test class distributions regarding the three class subsets.

In addition, since the imbalance degrees of the test datasets are relatively low on iNaturalist 2018, the simulated test class distributions are thus relatively balanced. As a result, the obtained performance improvement is not that significant, compared to other datasets. However, if there are more iNaturalist test samples following highly imbalanced test class distributions in real applications, our method would obtain more promising results.

Table 20: The performance improvement via test-time self-supervised aggregation on various test class distributions of ImageNet-LT, CIFAR100-LT, Places-LT and iNaturalist 2018.

Test Dist.	ImageNet-LT								CIFAR100-LT(IR10)							
	Ours w/o test-time aggregation				Ours w/ test-time aggregation				Ours w/o test-time aggregation				Ours w/ test-time aggregation			
	Many	Med.	Few	All	Many	Med.	Few	All	Many	Med.	Few	All	Many	Med.	Few	All
Forward-LT-50	65.6	55.7	44.1	65.5	70.0	53.2	33.1	69.4 (+3.9)	66.3	58.3	-	66.3	69.0	50.8	-	71.2 (+4.9)
Forward-LT-25	65.3	56.9	43.5	64.4	69.5	53.2	32.2	67.4 (+3.0)	63.1	60.8	-	64.5	67.6	52.2	-	69.4 (+4.9)
Forward-LT-10	66.5	56.8	44.2	63.6	69.9	54.3	34.7	65.4 (+1.8)	64.1	58.8	-	64.1	67.2	54.2	-	67.6 (+3.5)
Forward-LT-5	65.9	56.5	43.3	62.0	68.9	54.8	35.8	63.0 (+1.0)	62.7	57.1	-	62.7	66.9	54/3	-	66.3 (+3.6)
Forward-LT-2	66.2	56.5	42.1	60.0	68.2	56.0	40.1	60.6 (+0.6)	62.8	56.3	-	61.6	66.1	56.6	-	64.4 (+2.8)
Uniform	67.0	56.7	42.6	58.8	66.5	57.0	43.5	58.8 (+0.0)	65.5	59.9	-	63.6	65.8	58.8	-	63.6 (+0.0)
Backward-LT-2	66.3	56.7	43.1	56.8	65.3	57.1	45.0	57.1 (+0.3)	62.7	56.9	-	60.2	65.6	59.5	-	62.9 (+2.7)
Backward-LT-5	66.6	56.9	43.0	54.7	63.4	56.4	47.5	55.5 (+0.8)	62.8	57.5	-	59.7	65.1	60.4	-	62.4 (+2.7)
Backward-LT-10	65.0	57.6	43.1	53.1	60.9	57.5	50.1	54.5 (+1.4)	63.5	58.2	-	59.8	62.5	61.4	-	61.7 (+1.9)
Backward-LT-25	64.2	56.9	43.4	51.1	60.5	57.1	50.0	53.7 (+2.6)	63.4	57.7	-	58.7	61.9	62.0	-	62.1 (+3.4)
Backward-LT-50	69.1	57.0	42.9	49.8	60.7	56.2	50.7	53.1 (+3.3)	62.0	57.8	-	58.6	62.6	62.6	-	63.0 (+3.8)

Test Dist.	CIFAR100-LT(IR50)								CIFAR100-LT(IR100)							
	Ours w/o test-time aggregation				Ours w/ test-time aggregation				Ours w/o test-time aggregation				Ours w/ test-time aggregation			
	Many	Med.	Few	All	Many	Med.	Few	All	Many	Med.	Few	All	Many	Med.	Few	All
Forward-LT-50	59.7	53.3	26.9	59.5	68.0	44.1	19.4	67.2 (+7.7)	60.7	50.3	32.4	58.4	69.9	48.8	14.2	65.9 (+7.5)
Forward-LT-25	59.1	51.8	32.6	58.6	67.3	46.2	19.5	64.5 (+6.9)	60.6	49.6	29.4	57.0	68.9	46.5	15.1	62.5 (+5.5)
Forward-LT-10	59.7	47.2	36.1	56.4	67.2	45.7	24.7	61.2 (+4.8)	60.1	48.6	28.4	54.4	68.3	46.9	16.7	58.3 (+3.9)
Forward-LT-5	59.7	46.9	36.9	54.8	67.0	45.7	29.9	58.6 (+3.4)	60.3	50.3	29.5	53.1	68.3	45.3	19.4	54.8 (+1.7)
Forward-LT-2	59.2	48.4	41.9	53.2	63.8	48.5	39.3	55.4 (+2.2)	60.6	48.8	31.3	50.1	68.2	47.6	22.5	51.1 (+1.0)
Uniform	61.0	50.2	45.7	53.8	61.5	50.2	45.0	53.9 (+0.1)	61.6	50.5	33.9	49.4	65.4	49.3	29.3	49.8 (+0.4)
Backward-LT-2	59.0	48.2	42.8	50.1	57.5	49.7	49.4	51.9 (+1.8)	61.2	49.1	30.8	45.2	63.1	49.4	31.7	46.2 (+1.0)
Backward-LT-5	60.1	48.6	41.8	48.2	50.0	49.3	54.2	50.9 (+2.7)	62.0	48.9	32.0	42.6	56.2	49.1	38.2	44.7 (+2.1)
Backward-LT-10	58.6	46.9	42.6	46.1	49.3	49.1	54.6	51.0 (+4.9)	60.6	48.2	31.7	39.7	52.1	47.9	40.6	43.9 (+4.2)
Backward-LT-25	55.1	48.9	41.2	44.4	44.5	46.6	57.0	51.7 (+7.3)	58.2	47.9	32.2	36.7	48.7	44.2	41.8	42.5 (+5.8)
Backward-LT-50	57.0	48.8	41.6	43.6	45.8	46.6	58.4	52.8 (+9.2)	66.9	48.6	30.4	35.0	49.0	42.7	42.5	42.4 (+7.4)

Test Dist.	Places-LT								iNaturalist 2018							
	Ours w/o test-time aggregation				Ours w/ test-time aggregation				Ours w/o test-time aggregation				Ours w/ test-time aggregation			
	Many	Med.	Few	All	Many	Med.	Few	All	Many	Med.	Few	All	Many	Med.	Few	All
Forward-LT-50	43.5	42.5	65.9	43.7	46.8	39.3	30.5	46.4 (+2.7)	-	-	-	-	-	-	-	-
Forward-LT-25	42.8	42.1	29.3	42.7	46.3	38.9	23.6	44.9 (+2.3)	-	-	-	-	-	-	-	-
Forward-LT-10	42.3	41.9	34.9	42.3	45.4	39.0	27.0	43.3 (+1.0)	-	-	-	-	-	-	-	-
Forward-LT-5	43.0	44.0	33.1	42.4	45.6	40.6	27.3	42.6 (+0.2)	-	-	-	-	-	-	-	-
Forward-LT-2	43.4	42.4	32.6	41.3	44.9	41.2	29.5	41.3 (+0.0)	73.9	72.4	72.0	72.4	75.5	72.5	70.7	72.5 (+0.1)
Uniform	43.1	42.4	33.2	40.9	40.4	43.2	36.8	40.9 (+0.0)	74.4	72.5	73.1	72.9	74.5	72.5	73.0	72.9 (+0.0)
Backward-LT-2	42.8	41.9	33.2	39.9	37.1	42.9	40.0	40.6 (+0.7)	76.1	72.8	72.6	73.1	74.9	72.6	73.7	73.5 (+0.4)
Backward-LT-5	43.1	42.0	33.6	39.1	36.4	42.7	41.1	41.1 (+2.0)	-	-	-	-	-	-	-	-
Backward-LT-10	43.5	42.9	33.7	38.9	35.2	43.2	41.3	41.4 (+2.5)	-	-	-	-	-	-	-	-
Backward-LT-25	44.6	42.4	33.6	37.8	38.0	43.5	41.1	42.0 (+4.2)	-	-	-	-	-	-	-	-
Backward-LT-50	42.2	43.4	33.3	37.2	37.3	43.5	40.5	41.6 (+4.7)	-	-	-	-	-	-	-	-

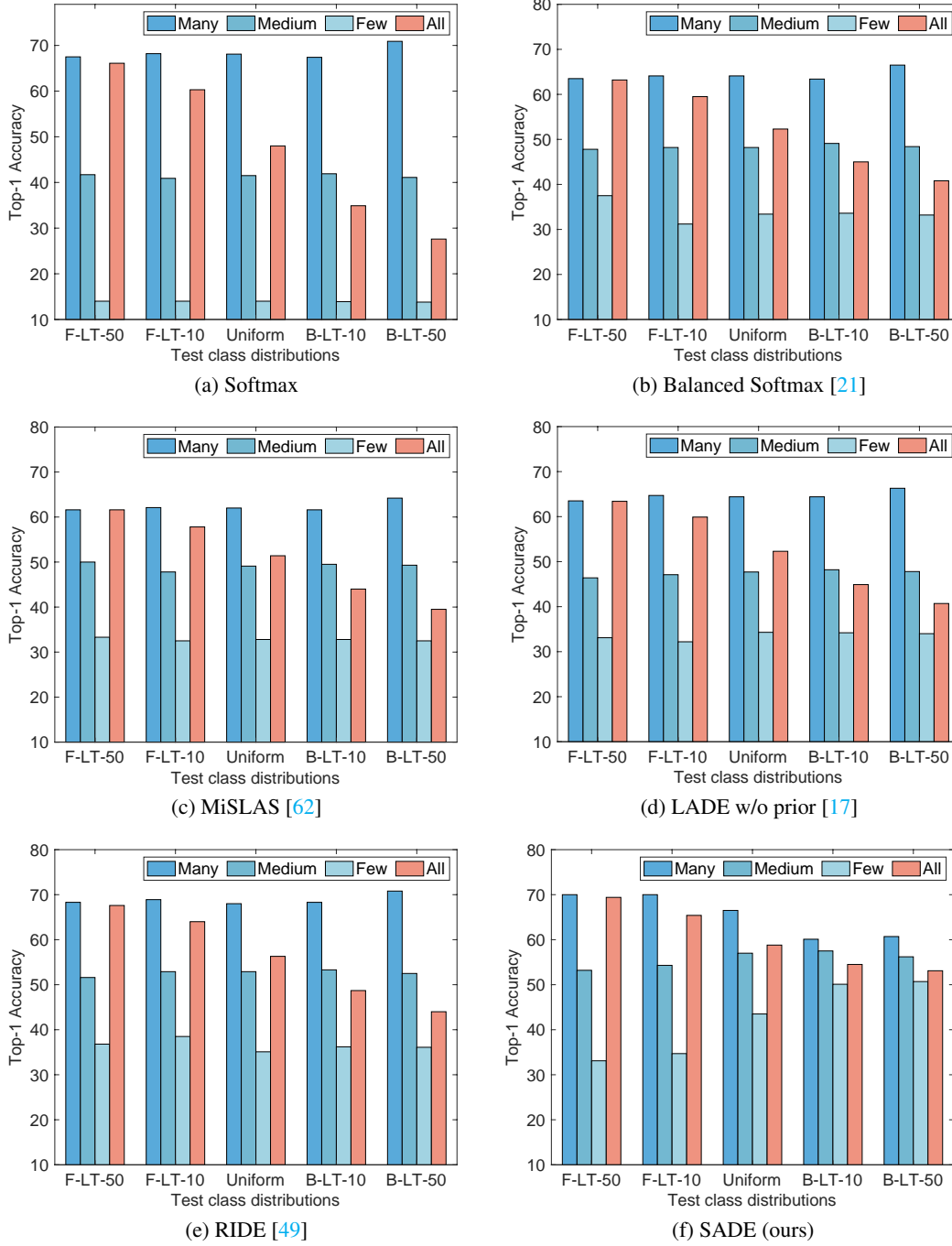


Figure 5: Top-1 accuracy of existing long-tailed (LT) methods on ImageNet-LT with various test class distributions, including uniform, forward and backward long-tailed ones with imbalance ratios 10 and 50, respectively. Here, “F-LT- N ” and “B-LT- N ” indicate the cases where test samples follow the same long-tailed distribution as training data and inversely long-tailed to the training data, with the imbalance ratio N , respectively. The results show that **existing methods perform very similarly on various test class distributions in terms of their performance on many-shot, medium-shot and few-shot classes**. In contrast, our proposed method is capable of adapting to various test class distributions in terms of many-shot, medium-shot and few-shot performance, thus leading to better overall performance on each test class distribution.

E Ablation Studies on Skill-diverse Expert Learning

E.1 Discussion on Expert Number

In SADE, we consider three experts, where the “forward” and “backward” experts are necessary since they span a wide spectrum of possible test class distributions, while the “uniform” expert ensures that we retain high accuracy on the uniform test class distributions. Nevertheless, our approach can be straightforwardly extended to more than three experts. For the models with more experts, we adjust the hyper-parameter λ in Eq. (3) for the new experts and keep the hyper-parameters of the original three experts unchanged, so that different experts are skilled in different types of class distributions. Following this, we further evaluate the influence of the expert number on our method based on ImageNet. To be specific, when there are four experts, we set $\lambda = 1$ for the new expert; while when there are five experts, we set $\lambda = 0.5$ and $\lambda = 1$ for the two newly-added experts, respectively. As shown in Table 21, with the increasing number of experts, the ensemble performance of our method is improved on vanilla long-tailed recognition, *e.g.*, four experts obtain a 1.2% performance gain compared to three experts on ImageNet-LT. As a result, our method with more experts obtains consistent performance improvement in test-agnostic long-tailed recognition on various test class distributions compared to three experts, as shown in Table 22. Even so, only three experts are sufficient to handle varied test class distributions, and provide a good trade-off between performance and efficiency.

Table 21: Performance of our method with different numbers of experts on ImageNet-LT with the uniform test distribution.

Model	4 experts				5 experts			
	Many-shot	Medium-shot	Few-shot	All classes	Many-shot	Medium-shot	Few-shot	All classes
Expert E_1	69.4	44.5	16.5	50.3	69.8	44.9	17.0	50.7
Expert E_2	66.2	51.5	32.9	54.6	68.8	48.4	23.9	52.9
Expert E_3	55.7	52.7	46.8	53.4	66.1	51.4	22.0	54.5
Expert E_4	44.1	49.7	55.9	48.4	56.8	52.7	47.7	53.6
Expert E_5	-	-	-	-	43.1	59.0	54.8	47.5
Ensemble	66.6	58.4	46.7	60.0	68.8	58.5	43.2	60.4

Table 22: Performance of our method with different numbers of experts on various test class distributions of ImageNet-LT.

Method	Experts	ImageNet-LT										
		Forward					Uniform	Backward				
		50	25	10	5	2	1	2	5	10	25	50
SADE	3 experts	69.4	67.4	65.4	63.0	60.6	58.8	57.1	55.5	54.5	53.7	53.1
	4 experts	70.1	68.1	66.3	64.2	61.6	60.0	58.7	57.6	56.7	56.1	55.6
	5 experts	70.7	68.9	66.8	64.5	62.1	60.4	58.7	57.2	56.3	55.6	54.7

E.2 Hyper-parameters in Inverse Softmax Loss

This appendix evaluates the influence of the hyper-parameter λ in the inverse softmax loss for the backward expert, where we fix all other hyper-parameters and only adjust the value of λ . As shown in Table 23, with the increase of λ , the backward expert simulates more inversely long-tailed distribution (to the training data), and thus the ensemble performance on *few-shot classes* is better. Moreover, when $\lambda \in \{2, 3\}$, our method achieves a better trade-off between head classes and tail classes, leading to relatively better overall performance on ImageNet-LT.

Table 23: Influence of the hyper-parameter λ in the inverse softmax loss on ImageNet-LT with the uniform test distribution.

Model	$\lambda = 0.5$			
	Many-shot classes	Medium-shot classes	Few-shot classes	All long-tailed classes
Forward Expert E_1	69.1	43.6	17.2	49.8
Uniform Expert E_2	66.4	50.9	33.4	54.5
Backward Expert E_3	61.9	51.9	40.3	54.2
Ensemble	71.0	54.6	33.4	58.0
Model	$\lambda = 1$			
	Many-shot classes	Medium-shot classes	Few-shot classes	All long-tailed classes
Forward Expert E_1	69.7	44.0	16.8	50.2
Uniform Expert E_2	65.5	51.1	32.4	54.4
Backward Expert E_3	56.5	52.3	47.1	53.2
Ensemble	77.2	55.7	36.2	58.6
Model	$\lambda = 2$			
	Many-shot classes	Medium-shot classes	Few-shot classes	All long-tailed classes
Forward Expert E_1	68.8	43.7	17.2	49.8
Uniform Expert E_2	65.5	50.5	33.3	53.9
Backward Expert E_3	43.4	48.6	53.9	47.3
Ensemble	67.0	56.7	42.6	58.8
Model	$\lambda = 3$			
	Many-shot classes	Medium-shot classes	Few-shot classes	All long-tailed classes
Forward Expert E_1	69.6	43.8	17.4	50.2
Uniform Expert E_2	66.2	50.7	33.1	54.2
Backward Expert E_3	43.4	48.6	53.9	48.0
Ensemble	67.8	56.8	42.4	59.1
Model	$\lambda = 4$			
	Many-shot classes	Medium-shot classes	Few-shot classes	All long-tailed classes
Forward Expert E_1	69.1	44.1	16.3	49.9
Uniform Expert E_2	65.7	50.8	32.6	54.1
Backward Expert E_3	21.9	38.1	58.9	34.7
Ensemble	60.2	57.5	50.4	57.6
Model	$\lambda = 5$			
	Many-shot classes	Medium-shot classes	Few-shot classes	All long-tailed classes
Forward Expert E_1	69.7	43.7	16.5	50.0
Uniform Expert E_2	65.9	50.9	33.0	54.2
Backward Expert E_3	16.0	33.9	60.6	30.6
Ensemble	56.3	57.5	54.0	56.6

F Ablation Studies on Test-time Self-supervised Aggregation

F.1 Influences of Training Epoch

As illustrated in Section 5.1, we set the training epoch of our test-time self-supervised aggregation strategy to 5 on all datasets. Here, we further evaluate the influence of the epoch number, where we adjust the epoch number from 1 to 100. As shown in Table 24, when the training epoch number is larger than 5, the learned expert weights by our method are converged on ImageNet-LT, which verifies that our method is robust enough. The corresponding performance on various test class distributions is reported in Table 25.

Table 24: The influence of the epoch number on the learned expert weights by test-time self-supervised aggregation on ImageNet-LT.

Test Dist.	Epoch 1			Epoch 5			Epoch 10		
	E1 (w_1)	E2 (w_2)	E3 (w_3)	E1 (w_1)	E2 (w_2)	E3 (w_3)	E1 (w_1)	E2 (w_2)	E3 (w_3)
Forward-LT-50	0.44	0.33	0.23	0.52	0.35	0.13	0.52	0.37	0.11
Forward-LT-25	0.43	0.34	0.23	0.50	0.35	0.15	0.50	0.37	0.13
Forward-LT-10	0.43	0.34	0.23	0.46	0.36	0.18	0.46	0.36	0.18
Forward-LT-5	0.41	0.34	0.25	0.43	0.34	0.23	0.43	0.35	0.22
Forward-LT-2	0.37	0.33	0.30	0.37	0.35	0.28	0.38	0.33	0.29
Uniform	0.34	0.31	0.35	0.33	0.33	0.34	0.33	0.32	0.35
Backward-LT-2	0.30	0.32	0.38	0.29	0.31	0.40	0.29	0.32	0.39
Backward-LT-5	0.27	0.29	0.44	0.24	0.31	0.45	0.23	0.31	0.46
Backward-LT-10	0.24	0.29	0.47	0.21	0.29	0.50	0.21	0.30	0.49
Backward-LT-25	0.23	0.29	0.48	0.18	0.29	0.53	0.17	0.3	0.53
Backward-LT-50	0.24	0.29	0.47	0.17	0.27	0.56	0.15	0.28	0.57

Test Dist.	Epoch 20			Epoch 50			Epoch 100		
	E1 (w_1)	E2 (w_2)	E3 (w_3)	E1 (w_1)	E2 (w_2)	E3 (w_3)	E1 (w_1)	E2 (w_2)	E3 (w_3)
Forward-LT-50	0.53	0.38	0.09	0.53	0.38	0.09	0.53	0.38	0.09
Forward-LT-25	0.51	0.37	0.12	0.52	0.37	0.11	0.50	0.38	0.12
Forward-LT-10	0.44	0.36	0.20	0.45	0.37	0.18	0.46	0.36	0.18
Forward-LT-5	0.42	0.35	0.23	0.42	0.35	0.23	0.42	0.35	0.23
Forward-LT-2	0.38	0.33	0.29	0.39	0.33	0.28	0.38	0.32	0.30
Uniform	0.33	0.33	0.34	0.34	0.32	0.34	0.32	0.33	0.35
Backward-LT-2	0.29	0.31	0.40	0.30	0.32	0.38	0.29	0.30	0.41
Backward-LT-5	0.24	0.31	0.45	0.23	0.29	0.48	0.25	0.30	0.45
Backward-LT-10	0.20	0.30	0.50	0.21	0.31	0.48	0.21	0.30	0.49
Backward-LT-25	0.16	0.30	0.54	0.17	0.29	0.54	0.17	0.30	0.53
Backward-LT-50	0.15	0.29	0.56	0.14	0.29	0.57	0.14	0.29	0.57

Table 25: The influence of the epoch number on the performance of test-time self-supervised aggregation on ImageNet-LT.

Test Dist.	Epoch 1				Epoch 5				Epoch 10			
	Many	Med.	Few	All	Many	Med.	Few	All	Many	Med.	Few	All
Forward-LT-50	68.8	54.6	37.5	68.5	70.0	53.2	33.1	69.4	70.1	52.9	32.4	69.5
Forward-LT-25	68.6	54.9	34.9	66.9	69.5	53.2	32.2	67.4	69.7	52.5	32.5	67.5
Forward-LT-10	60.3	55.3	37.6	65.2	69.9	54.3	34.7	65.4	69.9	54.5	35.0	65.4
Forward-LT-5	68.4	55.3	37.3	63.0	68.9	54.8	35.8	63.0	68.8	54.9	36.0	63.0
Forward-LT-2	67.9	56.2	40.8	60.6	68.2	56.0	40.1	60.6	68.2	56.0	39.7	60.5
Uniform	66.7	56.9	43.1	58.8	66.5	57.0	43.5	58.8	66.4	56.9	43.4	58.8
Backward-LT-2	65.6	57.1	44.7	57.1	65.3	57.1	45.0	57.1	65.3	57.1	45.0	57.1
Backward-LT-5	63.9	57.6	46.8	55.5	63.4	56.4	47.5	55.5	63.3	57.4	47.8	55.6
Backward-LT-10	62.1	57.6	47.9	54.2	60.9	57.5	50.1	54.5	61.1	57.6	48.9	54.5
Backward-LT-25	62.4	57.6	48.5	53.4	60.5	57.1	50.0	53.7	60.5	57.1	50.3	53.8
Backward-LT-50	64.9	56.7	47.8	51.9	60.7	56.2	50.7	53.1	60.1	55.9	51.2	53.2

Test Dist.	Epoch 20				Epoch 50				Epoch 100			
	Many	Med.	Few	All	Many	Med.	Few	All	Many	Med.	Few	All
Forward-LT-50	70.3	52.2	32.4	69.5	70.3	52.2	32.4	69.5	70.0	52.2	32.4	69.3
Forward-LT-25	69.8	52.4	31.4	67.5	69.9	52.3	31.4	67.6	69.7	52.6	32.6	67.5
Forward-LT-10	69.6	54.8	35.8	65.3	69.8	54.6	35.2	65.4	69.8	54.6	35.0	65.4
Forward-LT-5	68.7	55.0	36.4	63.0	68.	55.0	36.4	63.0	68.7	54.7	36.7	62.9
Forward-LT-2	68.1	56.0	39.9	60.5	68.3	55.9	39.6	60.5	68.2	56.0	40.1	60.6
Uniform	66.7	56.9	43.2	58.8	66.9	56.8	42.8	58.8	66.5	56.8	43.2	58.7
Backward-LT-2	65.4	57.1	44.9	57.1	65.6	57.0	44.7	57.1	64.9	57.0	45.6	57.0
Backward-LT-5	63.4	57.4	47.6	55.5	62.7	57.4	48.3	55.6	63.4	57.5	47.0	55.4
Backward-LT-10	60.7	57.5	49.4	54.6	61.1	57.6	48.8	54.4	60.6	57.6	49.1	54.5
Backward-LT-25	60.4	57.1	50.4	53.9	60.4	57.0	50.3	53.8	60.9	56.8	50.2	53.7
Backward-LT-50	60.9	56.1	51.1	53.2	60.6	55.9	51.1	53.2	60.8	56.1	51.2	53.2

F.2 Influences of Batch Size

In previous results, we set the batch size of test-time self-supervised aggregation to 128 on all datasets. In this appendix, we further evaluate the influence of the batch size on our strategy, where we adjust the batch size from 64 to 256. As shown in Table 26, with different batch sizes, the learned expert weights by our method keep nearly the same, which shows that our method is insensitive to the batch size. The corresponding performance on various test class distributions is reported in Table 27, where the performance is also nearly the same when using different batch sizes.

Table 26: The influence of the batch size on the learned expert weights by test-time self-supervised aggregation on ImageNet-LT.

Test Dist.	Batch size 64			Batch size 128			Batch size 256		
	E1 (w_1)	E2 (w_2)	E3 (w_3)	E1 (w_1)	E2 (w_2)	E3 (w_3)	E1 (w_1)	E2 (w_2)	E3 (w_3)
Forward-LT-50	0.52	0.37	0.11	0.52	0.35	0.13	0.50	0.33	0.17
Forward-LT-25	0.49	0.38	0.13	0.50	0.35	0.15	0.48	0.24	0.18
Forward-LT-10	0.46	0.36	0.18	0.46	0.36	0.18	0.45	0.35	0.20
Forward-LT-5	0.44	0.34	0.22	0.43	0.34	0.23	0.43	0.35	0.22
Forward-LT-2	0.37	0.34	0.29	0.37	0.35	0.28	0.38	0.33	0.29
Uniform	0.34	0.32	0.34	0.33	0.33	0.34	0.33	0.32	0.35
Backward-LT-2	0.28	0.32	0.40	0.29	0.31	0.40	0.30	0.31	0.39
Backward-LT-5	0.24	0.30	0.46	0.24	0.31	0.45	0.25	0.30	0.45
Backward-LT-10	0.21	0.30	0.49	0.21	0.29	0.50	0.22	0.29	0.49
Backward-LT-25	0.17	0.29	0.54	0.18	0.29	0.53	0.20	0.28	0.52
Backward-LT-50	0.15	0.30	0.55	0.17	0.27	0.56	0.19	0.27	0.54

Table 27: The influence of the batch size on the performance of test-time self-supervised aggregation on ImageNet-LT.

Test Dist.	Batch size 64				Batch size 128				Batch size 256			
	Many	Med.	Few	All	Many	Med.	Few	All	Many	Med.	Few	All
Forward-LT-50	70.0	52.6	33.8	69.3	70.0	53.2	33.1	69.4	69.7	53.8	34.6	69.2
Forward-LT-25	69.6	53.0	33.3	67.5	69.5	53.2	32.2	67.4	69.2	53.7	32.8	67.2
Forward-LT-10	69.9	54.3	34.8	65.4	69.9	54.3	34.7	65.4	69.5	55.0	35.9	65.3
Forward-LT-5	69.0	54.6	35.6	63.0	68.9	54.8	35.8	63.0	68.8	54.9	36.0	63.0
Forward-LT-2	68.2	56.0	40.0	60.6	68.2	56.0	40.1	60.6	68.1	56.0	40.1	60.5
Uniform	66.9	56.6	42.4	58.8	66.5	57.0	43.5	58.8	66.5	56.9	43.3	58.8
Backward-LT-2	64.9	57.0	45.7	57.0	65.3	57.1	45.0	57.1	65.5	57.1	44.8	57.1
Backward-LT-5	63.1	57.4	47.3	55.4	63.4	56.4	47.5	55.5	63.4	56.4	47.5	55.5
Backward-LT-10	60.9	57.7	48.6	54.4	60.9	57.5	50.1	54.5	61.3	57.6	48.7	54.4
Backward-LT-25	60.8	56.7	50.1	53.6	60.5	57.1	50.0	53.7	61.0	57.2	49.6	53.6
Backward-LT-50	61.1	56.2	50.8	53.1	60.7	56.2	50.7	53.1	61.2	56.4	50.0	52.9

F.3 Influences of Learning Rate

In this appendix, we evaluate the influence of the learning rate on our self-supervised strategy, where we adjust the learning rate from 0.001 to 0.5. As shown in Table 28, with the increase of the learning rate, the learned expert weights by our method are sharper and fit the unknown test class distributions better. For example, when the learning rate is 0.001, the weight for expert E_1 is 0.36 on the Forward-LT-50 test distribution, while when the learning rate increases to 0.5, the weight for expert E_1 becomes 0.57 on the Forward-LT-50 test distribution. Similar phenomenons are also observed on backward long-tailed test class distributions.

By observing the corresponding model performance on various test class distributions in Table 29, we find that when the learning rate is too small (e.g., 0.001), our test-time self-supervised aggregation strategy is unable to converge, given a fixed training epoch number of 5. In contrast, given the same training epoch, our method can obtain better performance by reasonably increasing the learning rate.

Table 28: The influence of the learning rate on the learned expert weights by test-time self-supervised aggregation on ImageNet-LT, where the number of the training epoch is 5.

Test Dist.	Learning rate 0.001			Learning rate 0.01			Learning rate 0.025		
	E1 (w_1)	E2 (w_2)	E3 (w_3)	E1 (w_1)	E2 (w_2)	E3 (w_3)	E1 (w_1)	E2 (w_2)	E3 (w_3)
Forward-LT-50	0.36	0.34	0.30	0.49	0.33	0.18	0.52	0.35	0.13
Forward-LT-25	0.36	0.34	0.30	0.48	0.34	0.18	0.50	0.35	0.15
Forward-LT-10	0.36	0.34	0.30	0.45	0.34	0.21	0.46	0.36	0.18
Forward-LT-5	0.36	0.33	0.31	0.43	0.34	0.23	0.43	0.34	0.23
Uniform	0.33	0.33	0.34	0.34	0.33	0.33	0.33	0.33	0.34
Backward-LT-5	0.31	0.32	0.37	0.25	0.31	0.44	0.24	0.31	0.45
Backward-LT-10	0.31	0.32	0.37	0.22	0.29	0.49	0.21	0.29	0.50
Backward-LT-25	0.31	0.32	0.37	0.21	0.28	0.51	0.18	0.29	0.53
Backward-LT-50	0.31	0.32	0.37	0.20	0.28	0.52	0.17	0.27	0.56

Test Dist.	Learning rate 0.05			Learning rate 0.1			Learning rate 0.5		
	E1 (w_1)	E2 (w_2)	E3 (w_3)	E1 (w_1)	E2 (w_2)	E3 (w_3)	E1 (w_1)	E2 (w_2)	E3 (w_3)
Forward-LT-50	0.53	0.36	0.11	0.53	0.37	0.10	0.57	0.34	0.09
Forward-LT-25	0.51	0.36	0.13	0.52	0.36	0.12	0.57	0.34	0.09
Forward-LT-10	0.45	0.37	0.18	0.47	0.36	0.18	0.44	0.36	0.20
Forward-LT-5	0.42	0.35	0.23	0.47	0.36	0.18	0.39	0.36	0.25
Uniform	0.33	0.33	0.34	0.31	0.31	0.38	0.33	0.34	0.33
Backward-LT-5	0.24	0.31	0.45	0.24	0.29	0.47	0.21	0.28	0.51
Backward-LT-10	0.21	0.30	0.49	0.21	0.31	0.48	0.22	0.32	0.46
Backward-LT-25	0.16	0.28	0.56	0.17	0.31	0.52	0.15	0.30	0.55
Backward-LT-50	0.15	0.28	0.57	0.14	0.28	0.58	0.12	0.27	0.61

Table 29: The influence of learning rates on test-time self-supervised aggregation on ImageNet-LT, under training epoch 5.

Test Dist.	Learning rate 0.001				Learning rate 0.01				Learning rate 0.025			
	Many	Med.	Few	All	Many	Med.	Few	All	Many	Med.	Few	All
Forward-LT-50	67.3	56.1	44.1	67.3	69.5	54.0	34.6	69.0	70.0	53.2	33.1	69.4
Forward-LT-25	67.4	56.2	40.3	66.1	69.2	53.8	33.2	67.2	69.5	53.2	32.2	67.4
Forward-LT-10	67.7	56.4	41.9	64.5	69.6	55.0	36.1	65.4	69.9	54.3	34.7	65.4
Forward-LT-5	67.2	55.9	40.8	62.6	68.7	55.0	36.2	63.0	68.9	54.8	35.8	63.0
Uniform	66.9	56.6	42.7	58.8	67.0	56.8	42.7	58.8	66.5	57.0	43.5	58.8
Backward-LT-5	65.8	57.5	43.7	55.0	63.9	57.5	46.9	55.5	63.4	56.4	47.5	55.5
Backward-LT-10	64.6	57.5	43.7	53.1	61.3	57.6	48.6	54.4	60.9	57.5	50.1	54.5
Backward-LT-25	66.0	57.3	44.1	51.5	61.1	57.4	49.3	53.5	60.5	57.1	50.0	53.7
Backward-LT-50	68.2	56.8	43.7	50.0	63.1	56.5	49.5	52.7	60.7	56.2	50.7	53.1

Test Dist.	Learning rate 0.05				Learning rate 0.1				Learning rate 0.5			
	Many	Med.	Few	All	Many	Med.	Few	All	Many	Med.	Few	All
Forward-LT-50	70.2	52.4	32.4	69.5	70.3	52.3	32.4	69.5	70.3	51.2	32.4	69.5
Forward-LT-25	69.7	52.5	32.5	67.5	69.9	52.3	31.4	67.6	69.9	51.1	29.5	67.5
Forward-LT-10	69.7	54.7	35.8	65.4	69.9	54.3	34.8	65.4	69.5	55.0	35.8	65.3
Forward-LT-5	68.8	54.9	36.2	63.0	68.8	54.8	36.1	63.0	68.3	55.3	37.6	62.9
Uniform	66.6	56.9	43.2	58.8	65.6	57.1	44.7	58.7	67.8	56.4	40.9	58.7
Backward-LT-5	63.6	57.5	48.9	55.4	63.0	57.4	48.1	55.6	61.4	57.4	49.2	55.6
Backward-LT-10	61.1	57.5	48.9	54.4	61.3	57.6	48.6	54.4	62.0	57.5	47.9	54.2
Backward-LT-25	59.9	56.8	51.0	53.9	60.9	57.2	49.9	53.7	60.2	56.8	50.8	53.9
Backward-LT-50	60.1	56.0	51.2	53.2	59.6	55.8	51.3	53.2	58.2	55.6	52.2	53.5

F.4 Results of Prediction Confidence

In our theoretical analysis (*i.e.*, Theorem 1), we find that our test-time self-supervised aggregation strategy not only simulates the test class distribution, but also makes the model predictions more confident. In this appendix, we evaluate whether our strategy can really improve the prediction confidence of models on various unknown test class distributions of ImageNet-LT. To this end, we compare the prediction confidence of our method without and with test-time self-supervised aggregation in terms of the hard mean of the highest prediction probability on all test samples.

As shown in Table 30, our test-time self-supervised aggregation strategy enables the deep model to have higher prediction confidence. For example, on the Forward-LT-50 test distribution, our strategy obtains 0.015 confidence improvement, which is non-trivial since it is an average value for a large number of samples (more than 10,000 samples). In addition, when the class imbalance ratio becomes larger, our method is able to obtain more apparent confidence improvement.

Table 30: Comparison of prediction confidence between our method without and with test-time self-supervised aggregation on ImageNet-LT, in terms of the hard mean of the highest prediction probability on each sample. The higher the highest prediction, the better the model.

Method	Prediction confidence on ImageNet-LT										
	Forward-LT					Uniform		Backward-LT			
	50	25	10	5	2	1	2	5	10	25	50
Ours w/o test-time aggregation	0.694	0.687	0.678	0.665	0.651	0.639	0.627	0.608	0.596	0.583	0.574
Ours w test-time aggregation	0.711	0.704	0.689	0.674	0.654	0.639	0.625	0.609	0.599	0.589	0.583

F.5 Run-time Cost of Test-time Aggregation

One may be interested in the run-time cost of our test-time self-supervised aggregation strategy, so we further report its running time on Forward-LT-50 and Forward-LT-25 test class distributions for illustration. As shown in Table 31, our test-time self-supervised aggregation strategy is fast in terms of per-epoch time. The actual average additional time is only 0.009 seconds per sample at test time on V100 GPUs. The result is easy to interpret since we freeze the model parameters and only learn the aggregation weights, which is much more efficient than training the whole model. More importantly, the goal of this paper is to handle a practical yet challenging test-agnostic long-tailed recognition task. For solving this challenging problem, we believe it is acceptable to allow models to be trained more, while the promising results in previous experiments have demonstrated the effectiveness of our proposed test-time self-supervised learning strategy in handling this problem. In the future, we will further extend the proposed method for better computational efficiency, *e.g.*, exploring dynamic network routing.

Table 31: Run-time cost of our test-time self-supervised aggregation strategy on ImageNet-LT, compared to the run-time cost of model training. Here, we show two test class distributions for illustration, which have different numbers of test samples.

Dataset	Model training	Test-time weight learning	
		Forward-LT-50	Forward-LT-25
Per-epoch time	713 s	110 s	130 s

F.6 Test-time Self-supervised Aggregation on Streaming Test Data

In the previous experiments, we conduct the test-time self-supervised aggregation strategy in an offline manner. However, as mentioned in Section 4.2, our test-time strategy can also be conducted in an online manner and does not require access to all the test data in advance. To verify this, we further conduct our test-time strategy on steaming test data of ImageNet-LT. As shown in Table 32, our test-time strategy performs well on the streaming test data. Even when the test data come in one by one, our test-time self-supervised strategy still outperforms the state-of-the-art baseline (i.e., offline Tent [46]) by a large margin.

Table 32: Results of our test-time self-supervised aggregation strategy on streaming test data of ImageNet-LT, where all test-time strategies are used on the same skill-diverse multi-expert model.

Backbone	Test-time strategy	Forward-LT		Backward-LT	
		50	5	5	50
SADE	No test-time adaptation	65.5	62.0	54.7	49.8
	Offline Tent [46]	68.0	62.8	53.2	45.7
	Offline self-supervised aggregation (ours)	69.4	63.0	55.5	53.1
	Online self-supervised aggregation with batch size 64	69.5	63.6	55.8	53.1
	Online self-supervised aggregation with batch size 8	69.8	63.0	55.4	53.0
	Online self-supervised aggregation with batch size 1	69.0	62.8	55.2	52.8

G More Discussions on Model Complexity

In this appendix, we discuss the model complexity of our method in terms of the number of parameters, multiply-accumulate operations (MACs) and top-1 accuracy on test-agnostic long-tailed recognition. As shown in Table 33, both SADE and RIDE belong to ensemble-based long-tailed learning methods, so they have more parameters (about 1.5x) and MACs (about 1.4x) than the original backbone model, where we do not use the efficient expert assignment trick in [49] for both methods. Because of the ensemble effectiveness of the multi-expert scheme, both methods perform much better than non-ensemble methods (*e.g.*, Softmax and other long-tailed methods). In addition, since our method and RIDE use the same multi-expert framework, both methods have the same number of parameters and MACs. Nevertheless, by using our proposed skill-diverse expert learning and test-time self-supervised aggregation strategies, our method performs much better than RIDE with no increase in model parameters and computational costs.

One may concern the multi-expert scheme leads to more model parameters and higher computational costs than the original backbone. However, note that the main focus of this paper is to solve the challenging test-agnostic long-tailed recognition, while promising results have shown that our method addresses this problem well. In this sense, slightly increasing the model complexity is acceptable for solving this practical yet challenging problem. Moreover, since there have already been many studies [14, 51] showing effectiveness in improving the efficiency of the multi-expert scheme, we think the computation increment is not a severe issue and we leave it to the future.

Table 33: Model complexity and performance of different methods in terms of the parameter number, Multiply-Accumulate Operations (MACs) and top-1 accuracy on test-agnostic long-tailed recognition. Here, we do not use the efficient expert assignment trick in [49] for RIDE and our method.

			ImageNet-LT (ResNeXt-50)										
Method	Params (M)	MACs (G)	Forward-LT					Uniform	Backward-LT				
			50	25	10	5	2	1	2	5	10	25	50
Softmax	25.03 (1.0x)	4.26 (1.0x)	66.1	63.8	60.3	56.6	52.0	48.0	43.9	38.6	34.9	30.9	27.6
RIDE [49]	38.28 (1.5x)	6.08 (1.4x)	67.6	66.3	64.0	61.7	58.9	56.3	54.0	51.0	48.7	46.2	44.0
SADE (ours)	38.28 (1.5x)	6.08 (1.4x)	69.4	67.4	65.4	63.0	60.6	58.8	57.1	55.5	54.5	53.7	53.1
CIFAR100-LT-IR100 (ResNet-32)													
Method	Params (M)	MACs (G)	Forward-LT					Uniform	Backward-LT				
			50	25	10	5	2	1	2	5	10	25	50
Softmax	0.46 (1.0x)	0.07 (1.0x)	63.3	62.0	56.2	52.5	46.4	41.4	36.5	30.5	25.8	21.7	17.5
RIDE [49]	0.77 (1.5x)	0.10 (1.4x)	63.0	59.9	57.0	53.6	49.4	48.0	42.5	38.1	35.4	31.6	29.2
SADE (ours)	0.77 (1.5x)	0.10 (1.4x)	65.9	62.5	58.3	54.8	51.1	49.8	46.2	44.7	43.9	42.5	42.4
Places-LT (ResNet-152)													
Method	Params (M)	MACs (G)	Forward-LT					Uniform	Backward-LT				
			50	25	10	5	2	1	2	5	10	25	50
Softmax	60.19 (1.0x)	11.56 (1.0x)	45.6	42.7	40.2	38.0	34.1	31.4	28.4	25.4	23.4	20.8	19.4
RIDE [49]	88.07 (1.5x)	13.18 (1.1x)	43.1	41.8	41.6	42.0	41.0	40.3	39.6	38.7	38.2	37.0	36.9
SADE (ours)	88.07 (1.5x)	13.18 (1.1x)	46.4	44.9	43.3	42.6	41.3	40.9	40.6	41.1	41.4	42.0	41.6
iNaturalist 2018 (ResNet-50)													
Method	Params (M)	MACs (G)	Forward-LT		Uniform		Backward-LT						
			3	2	1	2			3				
Softmax	25.56 (1.0x)	4.14 (1.0x)	65.4	65.5	64.7	64.0	63.4						
RIDE [49]	39.07 (1.5x)	5.80 (1.4x)	71.5	71.9	71.8	71.9	71.8						
SADE (ours)	39.07 (1.5x)	5.80 (1.4x)	72.3	72.5	72.9	73.5	73.3						

H Potential Limitations

One concern is that this work only focuses on long-tailed classification problems. However, we believe this is enough for a new challenging task of test-agnostic long-tailed recognition, while how to extending to object detection and instance segmentation will be explored in the future. Another potential concern is the model complexity of our method. However, as discussed in Appendix G, the computation increment is not a very severe issue, while how to further accelerate our method will be explored in future. In addition, one may also expect to evaluate the proposed method on more test class distributions. However, as shown in Section 5.3, we have demonstrated the effectiveness of our method on the uniform class distribution, the forward and backward long-tailed class distributions with various imbalance ratios, and even partial class distributions. Therefore, we believe the empirical verification is sufficient for verifying our method, and the extension to more complex test class distributions is left to the future.